Tisk této publikace byl podpořen z projektu:
„Tvorba mezinárodního vědeckého týmu a zapojování do vědeckých sítí v oblasti nanotechnologií a nekonvenčního tváření materiálu“, reg. č. CZ.1.07/2.3.00/20.0038
podporovaného Operačním programem Vzdělávání pro konkurenceschopnost, spolufinancovaného z Evropského sociálního fondu a ze státního rozpočtu České republiky.

Autor:	kolektiv autorů
Pracoviště:	VŠB-Technická univerzita Ostrava Fakulta strojní
Název:	Sborník příspěvků z workshopu „New Trends“
Místo, rok:	Ostrava, 2014
Počet stran:	70
Vydala:	Vysoká škola báňská – Technická univerzita Ostrava, FS, Katedra mechanické technologie

Za obsah příspěvků odpovídají jednotliví autoři.

Vysoká škola báňská – Technická univerzita Ostrava, 2014

ISBN 978-80-248-3475-7

Nanotým VŠB – TU Ostrava
CZ.1.07/2.3.00/20.0038

INVESTICE DO ROZVOJE VZDĚLÁVÁNÍ

Nanotým VŠB – TU Ostrava

CZ.1.07/2.3.00/20.0038

WORKSHOP

„New Trends“

21. – 23. února 2013

Sborník příspěvků

Interhotel TATRA, Kopřivnice, Česká republika
2013

Project name:	Creation of an international team of scientists and participation in scientific networks in the sphere of nanotechnology and unconventional forming material.
Program:	Operational Programme Education for Competitiveness
Priority Programme:	2 - Tertiary Education, Research and Development
Support area:	2.3 - Human resources in research and development
Registration number:	CZ.1.07/2.3.00/20.0038
Project start date:	1. June 2011
Project closing date:	31. May 2014
Project applicant:	VŠB - TU Ostrava
Project partner:	COMTES FHT a.s.
Administrative team:	Main project manager – prof. Ing. Stanislav Rusz, CSc. Project coordinator – Ing. Jan Kedroň Finance manager – Ing. Stanislav Tylšar

Nanoteam VSB – TU Ostrava
CZ.1.07/2.3.00/20.0038

WORKSHOP
„New trends“

Proceedings

21st – 23rd February 2013
Interhotel TATRA
Kopřivnice, Czech Republic

VŠB – Technical University of Ostrava, Faculty of Mechanical Engineering, Department of Mechanical Technology, 2014

european social fund in the czech republic
EUROPEAN UNION
MINISTRY OF EDUCATION, YOUTH AND SPORTS
OP Education for Competitiveness
INVESTMENTS IN EDUCATION DEVELOPMENT

Evaluation of sheet-metal strain by embossed circular grids

Radek ČADA

VŠB – Technical University of Ostrava, 17. Listopadu 15, CZ 708 33 Ostrava-Poruba, Czech Republic, radek.cada@vsb.cz

Abstract

Contribution concerns the method of deformation networks in range of sheet-metal forming. Principle of this method consist in creation of deformation network at sheet-metal blank before forming and evaluation of its deformation at any moment or after forming operation in forming tool.

A special apparatus for embossing of circular grids on sheets with continuous regulation of embossing force was constructed. With this apparatus accurate, clear and permanent circles can be applied to the sheet simply, very quickly, without the use of a power source. The apparatus has small dimensions and so it is portable, its cost is low.

At drawing of intricate shape stampings from steel deep-drawing sheets the using of impression depths between 0.05 mm and 0.06 mm proved true, which guarantee minimum sheet-metal influence by deformation in places of impressions with contemporaneous good legibility even after great plastic deformation of material.

Keywords

Deformation network, sheet-metal, circular grid, embossing, strain, forming.

1 INTRODUCTION

Often during a forming operation certain areas of the sheet-metal undergo a complicated sequence of plastic deformation. A particular sheet of metal can be formed without breakage depends on material properties, surface conditions, blank size and shape, lubrication, press speed, blankholder pressure, punch and die design, and many other known and unknown factors. The amount of deformation determines when sheet-metal will fail.

Areas of the sheet that are subject to the greatest deformation and which are the most likely areas of breakage are made visible by making of straight lines or circles on the blank, then forming the part.

Strain patterns are clearly visible after forming. If the sheet is thin, they indicate the strain through the thickness of the sheet.

2 EVALUATION OF STRAIN AND MATERIAL FLOW IN STAMPINGS

2.1 Circular grid system

An ideal grid system is non-directional. A circle is always correctly oriented to furnish the maximum strains directly.

When the material is strained, the circle becomes an ellipse. The two principal strain directions are vividly indicated by the major and minor axes of the ellipse. Further, by measuring the major and minor axes and comparing with the original circle diameter, the relative strain in each direction is readily determined. The onset of fracture in the principal axis of strain is governed by the degree of stretching in both the major and minor axes.

By examining a number of pressings and deep drawings exhibiting failure, limiting strain curves may be constructed for each material in use. Subsequently, the strain values for a new pressing or deep drawing may be referred to the graph and the reliability of the unit readily predicted.

The grid-marking system provides a most useful method for identifying critical zones of deformation on difficult workpieces. Measurements and visualization of strain patterns make possible to locate and eliminate the causes of many breakage problems.

When working in the limiting zones of deformation where there is a danger of necking or the formation of cracks, it is possible by step-by-step analysis to identify critical points so that appropriate measures can be taken.

Thus, this basically empirical method, is an aid to optimising, at minimum cost, the manufacture of, and the manufacturing technique for, the production of high-quality components.

2.2 Evaluation of deformations at forming

It is possible to evaluate the changes of deformation network after forming from many points of view and by various manners, from the simplest to the intricatest.

The values of main strains can be calculated from formulae:

$$\varepsilon_1 = \frac{L_1 - L_0}{L_0} \cdot 100 \quad (\%) \tag{1}$$

$$\varepsilon_2 = \frac{L_2 - L_0}{L_0} \cdot 100 \quad (\%) \tag{2}$$

where L_0 is the initial diameter of circle element, L_1 is the length of main axis of ellipse, L_2 is the length of secondary axis of ellipse (see Fig. 1).

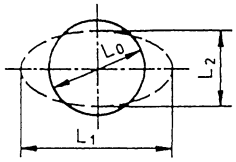

Fig. 1 Circular element of deformation network before forming (solid line) and after forming (dash line)

The values of main logarithmic deformations:

$$\varphi_1 = \ln \frac{L_1}{L_0} = \ln\left(1+\varepsilon_1\right) \tag{3}$$

$$\varphi_2 = \ln \frac{L_2}{L_0} = \ln\left(1+\varepsilon_2\right) \tag{4}$$

$$\varphi_3 = -\varphi_1 - \varphi_2 \tag{5}$$

From the volume conservation law in the place of deformation network element the sheet-metal thickness in this place after forming process can be calculated.

Deformation network circular element area before forming:

$$S_0 = \frac{\pi \cdot L_0^2}{4} \tag{6}$$

The area of the deformation network element after forming, i. e. the area of ellipse:

$$S = \pi \cdot L_1 \cdot L_2 \tag{7}$$

The law of volume conservation in the place of deformation network element:

$$S_0 \cdot s_0 = S \cdot s \tag{8}$$

Sheet-metal thickness of in the place of deformation network element after forming:

$$S = \frac{S_0 \cdot L_0^2}{4 \cdot L_1 \cdot L_2} \tag{9}$$

2.3 Methods of grid marking

It is possible to make circular grids by photographic method [1, 2], printing (serigraphy [3, 4], offset [1], rubber stereotyping [1]), chemical etching [5], electrolytic etching [6], electroerosive sparker [1], graving [1] and embossing [7].

The differences among separate methods of circular grids making are in drawing thickness, reproduction accuracy, possibility to make network with small parameters, legibility after great plastic deformation, etc.

Every method, mentioned above, do not offer at practical use only advantages. That is why every method has its chracteristic and suitable use in practice.

The generally valid principle is, that such method of making circular grids is to be used, which guarantees getting of network with required quality and minimal cost.

3 GRID MARKING BY EMBOSSING

3.1 Old methods

The original method of making circular grids by embossing consists in using cylindrical

embossing punch without head [7]. A cylindrical metal peace was used for guarantee the embossing punch perpendicularity to the sheet-metal plane.

The principal disadvantage of this method consisted in the fact, that it was not possible to regulate the impression depth, so it was not possible to guarantee making of certain number of absolutely uniform impressions. At making grids on thin sheets a great local plastic deformation and arising of notches occured in places of deeper impressions.

The disadvantages, mentioned above, were removed by constructing of jig for embossing of circular grids (see Fig. 2), which consists of two main parts – head and basic body, which are joined by thread. The embossing punch has a stop head in its upper part.

Using of this jig has shown, that it would be useful to regulate the impression depth with greater accuracy. So aditionally a special apparatus for embossing of circular grids (see Fig. 3) was constructed. This apparatus is author's invention (CZ Patent No. 265048).

This apparatus consists of three main parts – head, central screw-nut and basic body, which are joined by threads with different lead [7]. The embossing punch has a stop contact surface in its upper part.

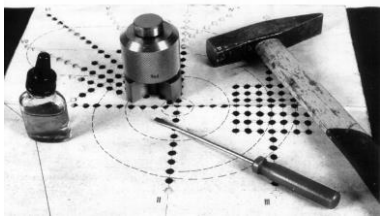

Fig. 2 Jig for embossing of circular grids on paper template for grid marking

Fig. 3 Special apparatus for embossing of circular grids with central screw nut

3.2 Method by special apparatus for grid marking

Additionally the apparatus for making circular grids on sheets with continuous regulation of embossing force (Fig. 4) has been constructed, which the author applied for a patent at the Office of Industrial Proprietorship in Prague in Czech Republic.

The apparatus consists of basic body, on which the central screw-nut is mounted by thread and on it the head is mounted by thread with different lead.

After assembly of apparatus the head and basic body are locked against angular displacement by two screws in head the ends of them fall into vertical slots in basic body and by that the axial motion of head towards basic body at moving round a slight amount of central screw-nut is made possible. The central screw-nut has on its surface knurling for function of scale at change of impression depth adjustment.

By suitable selected difference of threads lead in apparatus head and in basic body it is possible to achieve arbitrary fineness regulation of the whole apparatus height and by that regulation of the depth of impression.

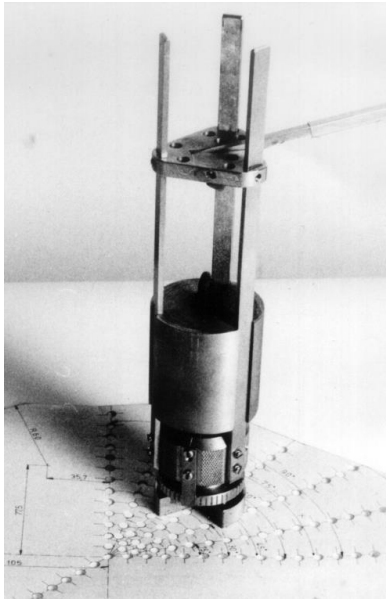

Fig. 4 Special apparatus for grid marking with continuous regulation of embossing force

The change largeness of the whole apparatus height up to one turning of central screw-nut is divided into definite number of sections. Every section is up to definite equal angle of turning of central screw-nut. By suitable Selected external diameter of central screw-nut it is possible to use knurlink for making scale lines. Separate scale lines of the central screw-nut are put out under edge of arm, which is fastened to apparatus head by two screws. After putting out the whole apparatus height it is possible to fix the position of central screw-nut by three fixation screws in basic body. The apparatus head has a stop contact surface for stop contact surface of the embossing punch. On periphery of head the vertical guide gibs are fastened, on which the traverser fitted with fixation screws for setting of its height above the head is mounted. The traverser has lock for clamping of yoke of drop weight, which is slidingly mounted among the vertical guide gibs. One guide gib is fitted with numerical scale for possibility of reading of traverser height above the head. The embossing punch with stop contact surface in upper part is the tool. The embossing force is induced by free fall of drop weight on the head of embossing punch.

3.3 Properties of the apparatus

The apparatus for embossing of circular grids guarantees perpendicularity of embossing tool to the sheet-metal plane and by that uniform impression of the whole embossing tool edge shape, it makes possible to regulate steplessly the impression depth with accuracy of ± 0,01 mm. The apparatus makes possible an exact establishing on required place of future impression, which has been marked on sheet-metal plane in advance, with the use of lower edges of rectangular slot in basic body and simultaneously with the use of two lines on periphery of lower part of basic body.

The apparatus guarantees action of the embossing force in the axis of embossing punch, makes possible to regulate finely its intensity and makes possible to set up the constant intensity of it for definite number of impressions.

With the described apparatus accurate, clear and permanent circles can be applied to the sheet simply, very quickly, without the use of a power source. The apparatus has small dimensions and so it is portable, its cost is low.

At drawing of intricate shape stampings from steel deep-drawing sheets (Fig. 5 and Fig. 6) the using of impression depths between 0.05 mm and 0.06 mm proved true, which guarantee minimum sheet-metal influence by deformation in places of impressions with contemporaneous good legibility even after great plastic deformation of material.

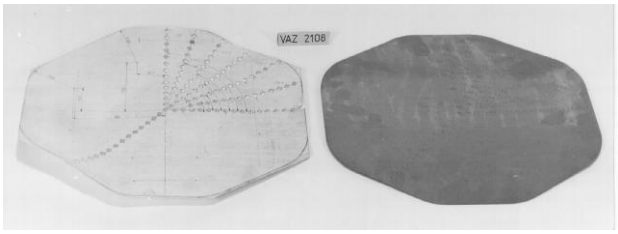

Fig. 5 Paper template for embossing and blank for drawing of stampings of oval paraboloid headlamp reflector for automobile VAZ 2108

Fig. 6 Stampings of oval paraboloid headlamp reflector for automobile VAZ 2108 after 1st, 2nd and 3rd forming operation with deformation networks made by embossing

No evidence has been accumulated which would suggest that embossing circular grids by special apparatus, mentioned above, causes premature failure in pressing and studies of fractures do not suggest that they initiate from a mark or propagate along them.

4 REFERENCES

[1] VESELÝ, M. Atlas informací pro uživatele tenkých plechů – III. díl. Praha: Výzkumný ústav strojírenské technologie a ekonomiky, 1972. 260 s.

[2] LARSEN, B. Photo-Chemical Etching of Circular Grids. Sheet Metal Industries, No. 3, 1974, pp. 139-142. ISSN 0037-3435.

[3] RIVENAES, U. Simple and Cheap Gridmarking. Sheet Metal Industries, No. 3, 1974, pp. 132-138. ISSN 0037-3435.

[4] KOŘÍNEK, M. a MIKEŠ, V. Zjišťování napjatosti a přetvoření na výliscích nepravidelných tvarů. Strojírenství, No. 1, 1966, pp. 59-62.

[5] ŠANOVEC, J., PORTUŽÁKOVÁ, V. a ROLLER, I. Zaleptané sítě k zjišťování intenzity přetvoření při tváření zastudena. Strojírenská výroba, No. 2, 1973, pp. 104-106. ISSN 0039-2456.

[6] WELCH, E. H. Gridmarking Helps Solve Forming Problems in Aluminium. Sheet Metal Industries, No. 3, 1974, pp. 135-138. ISSN 0037-3435.

[7] ČADA, R. Embossed circular grid system in sheet-metal forming. In: 2nd International Conference "NON-FERROUS METALS '95". Poland, Kraków: Akademia Górniczo-Hutnicza, 1995, s. 365-368. ISBN 83-904497-0-6.

Acknowledgement

This paper was created within the project No. **CZ.1.07/2.3.00/20.0038** with the name ***"Creation of an international scientific team and incorporation to scientific networks in the area of nanotechnologies and material unconventional forming"***, which is financed by the European Social Fund and state budget of the Czech Republic. Results in the paper were achieved at solving of specific research project No. **SP2013/63** with the name ***"Optimization of Flat and Volume Forming Technologies"*** solved in year 2013 at Faculty of Mechanical Engineering of VŠB – Technical University of Ostrava.

european social fund in the czech republic
EUROPEAN UNION
MINISTRY OF EDUCATION, YOUTH AND SPORTS
OP Education for Competitiveness
INVESTMENTS IN EDUCATION DEVELOPMENT

Tixoforming of steels

J. Dutkiewicz, L. Rogal

Institute of Metallurgy and Materials Science of the Polish Academy of Sciences Kraków ul. Reymonta 25

1. INTRODUCTION

Semi-solid metal (SSM) processing was developed at MIT in the early 1970s [1]. SSM uses thixotropic flow of semi-solid slurry [2]. The system is described as thixotropic when a reduction in magnitude of its rheological properties, such as elastic modulus, yield stress and viscosity occur reversibly and isothermally with a distinct time dependence on shear strain applied [3,4]. A metal alloy can behave in a thixotropic way if it has a wide temperature range of solidus-liquidus and a globular microstructure within this range. The applied amount of liquid phase is usually from 20%-60% and depends on the type of process [4,5,6]. Globular microstructure for the semi-solid process is produced depending on the process types; thixo-process using a reheating of a previously prepared billet and rheo-process which starts directly from the melt. Semi-solid metal processing is an alternative method of forming metal alloys for casting and forging [6].Today, rheoforming and thixoforming of Al-base, Zn-base and Mg-base alloys find common applications an industry[7,8,9]. In a case of high melting alloys such as steel and titanium there exist a lot of restrictions referring to a die material, strong oxidation of feedstock and temperature control [10]. In spite of these difficulties, a prototype device for a serial production of steel thixo-casts was built in Krakow [11]. High cost of feedstock manufacture is also an obstacle to a widespread application. As a result steel thixoforming can be applied only in the case when forging and casting cannot be used [12]. Until now several steels e.g. D2, M2, C38, C45, 16MnCr5, 100Cr6, 304 stainless steel, HP/9/4/30 in application for SSM have been investigated [13-17]. The hypoeutectic chromium X210CrW12 steel is very interesting from the point of view of SSM forming as it has: a wide range of solidus-liquidus, low sensitivity to temperature changes in the semi-solid state, relatively low process temperature [16]. Globular microstructure is produced by Strain Induced and Melt Activated SIMA and Recrystallization Activated Process RAP for thixo-process and by slope induced flow and modification of chemical composition by grain refiners for rheo-process [18]. The presence of a high amount of carbides is responsible for a decrease of the grain growth during heating to a semi-solid state [1-2]. Microstructure after semi-solid processing consists of austenitic globular grains (average size 46 μm) surrounded by eutectic mixture. The X210CrW12 thixo-cast after direct processing does not have a practical application due to its low hardness and a poor resistance to wear. The present paper focuses on the investigation of the microstructure of cutter teeth thixo-casts directly after the thixoforming process and the influence of a different heat treatment conditions on the thixo-cast microstructure and its mechanical properties.

2. EXPERIMENTAL PROCEDURE

2.1 Material

The X210CrW12 tool steel used was produced by Batory Steel Works S.A. in Poland. The steel was hot rolled at approximately 1050°C; next it was annealed at 840°C and subsequently stress-relief annealed at 650°C. The chemical composition was 2,1 %C, 10,5 %Cr, 0,7 %W, 0,4 %Si, 0,4 - Mn (all in weight %). A calculated temperature versus mass % C phase diagram for compositions near investigated tool steel with variable carbon content after [6] is shown in Fig 1. A thick dotted line marks the content of carbon corresponding to X210CrW12 steel.

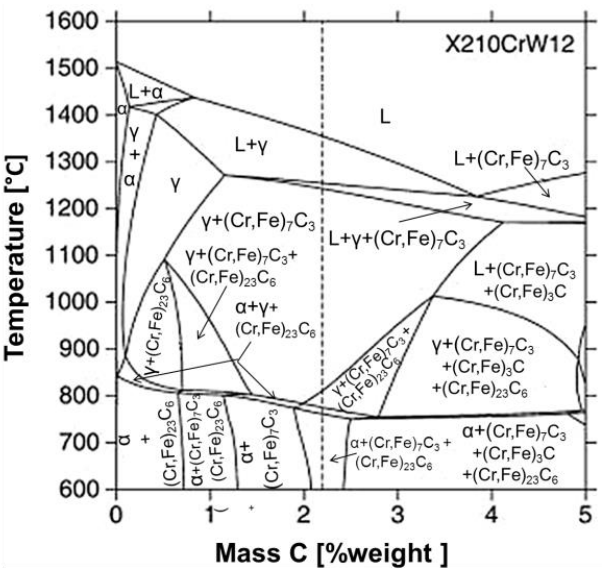

Fig. 1 a) Calculated section of a pseudo-binary phase diagram for compositionnear X210CrW12 steel with variable C content [6]. The dashed lines show content of carbon corresponding to X210CrW12 steel.

2.2 Calorimetric and dilatometric analysis

DuPont910 (up to 665°C), SDT Q600 TA Instruments (up to 1000°C) and Netzsch (up to 1550°C) were used to measure thermal effects during heating and cooling at the rate of 30°C/min in helium atmosphere. Dilatometric tests were performed with the Adamel DT1000 dilatometer for determination of temperature of phase transformation [11]. The samples of 2x12 mm were heated with the rate of 30°C/min up to 1000°C, at Argon atmosphere.

2.3 Thixoforming procedure

Thixo-cast of main bucket tooth thixo-cast were made using a specially built prototype device. The piston velocity of 1 m/s was applied. The locking force of the machine was 800 kN. A billet (diameter – 30 mm, height – 30 mm) of X210CrW12 steel was placed in the coil of an inductive heating furnace. The temperature of feedstock was measured by S type thermocouple. The billet was then moved to a cylinder of a high-pressure die-casting machine and pressed out by a piston into the die, made of M2 steel, pre-heated to 150ºC and covered with BN.

3. RESULTS OF OWN RESEARCH

3.1 Starting material

The X210CrW12 steel with a high content of chromium and carbon belongs to the ledeburite class of steels due to primary carbides precipitates during solidification before the eutectic. During hot rolling the eutectic is broken, which results in a longitudinal direction of the ingot (Fig. 1). After complex heat treatment; annealing and tempering it acquires a ferritic structure with undissolved carbides. Figure 2 shows a scanning electron micrograph with back-scattered electron imaging mode for the as-received X210CrW12 tool steel. It shows a primary carbide precipitation in the ferrite/pearlite matrix formed in bands parallel to the working direction. EDS analysis of matrix (point 1, Figure 1a) is as follows: 1,9 % C, 18,1 % Cr, 0,7 % Mn, 1,8 % W, 0,3 % V 0,3 % Si 76,9 % Fe. The chemical composition analysis of primary carbides (point (2), chromium carbides, (3) tungsten carbides in Figure 1a) are as follows (2); 3,7%, C 44,5%,Cr 0,1%Si, 0,8%Mn, 1,3%W, 0,8%V, 48,8% Fe and (3) 1.9%C, 12%,Cr 0,2%Si, 0,9%Mn, 6,3%W, 78,7%Fe. The average hardness of the billet is 220 HV_5. Such steel was used as a feedstock for the thixoforming process.

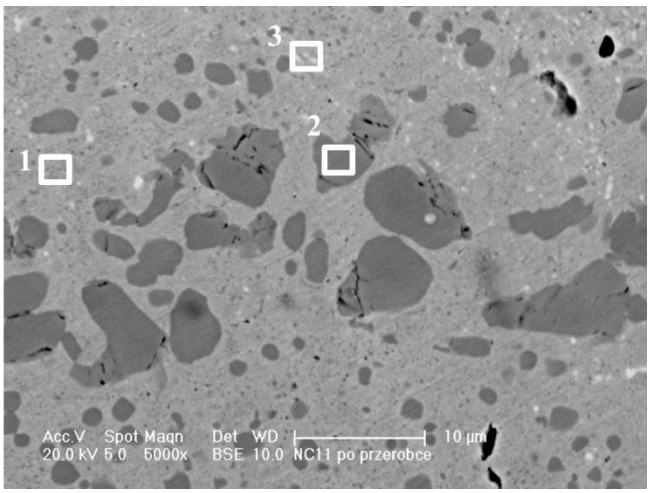

Fig. 2 SEM microstructure of X210CrW12 steel after rolling – feedstock for thixoforming

In Figure 3 the DSC curve (1) shows the endothermic effects, which occurred during heating at the rate of 20°C/ min. The curve (2) in Figure 2 shows the dependence of the calculated amount of liquid phase as a function of temperature. The melting point is determined as the onset of the endothermic peak. The start of the melting is set at such temperature when the heat curve falls away from the tangent line. The end of the melting is set by the onset point on the other side of the peak. A strong endothermic effect begins at 1207°C and ends at 1377°C. The enthalpy of the melting process is 612 J/g. The analysis of the melting curve shows that in the range 1207°C - 1255°C (0-40% liquid phase) the enthalpy of melting is much larger than during the rest of the process. This effect is connected with the melting of the eutectic. Over 1255 °C mainly solid solution melts. This effect is also observable in the curve(2) which shows different kinetics of changes of the amount of liquid phase as a function of the temperature. Semi-solid processing was carried out at 1250°C which corresponds to 38% of liquid phase in accordance with DSC-DTA analysis (point A marked in Fig 3). The amount of liquid phase was also determined as 38% on the basis of the content of the eutectic phase in the thixo-cast microstructure. The discrepancy in the volume liquid

phase results from different heating rates as well as inhomogeneous chemical composition of feedstock.

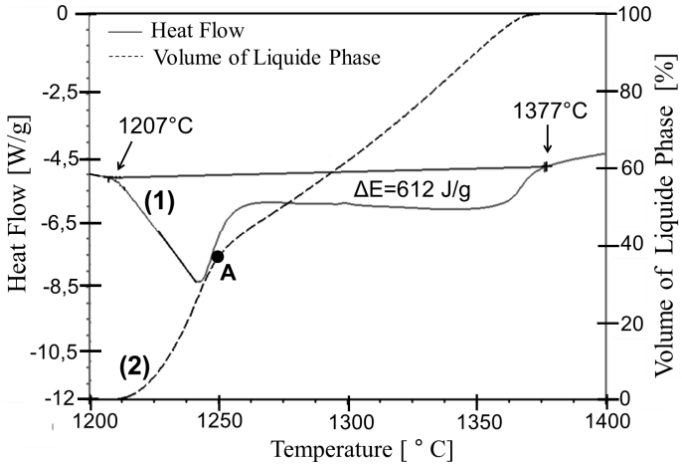

Fig. 3 DSC-TGA heating curve for X210CrW12 steel after rolling

3.2 Thixo-casts analysis

The main bucket tooth thixo-casts made of X210CrW12 steel are presented in Fig. 4a. A precise reproduction of a die shape without visible surface defects of thixo-casts was obtained. The average hardness of the thixo-casts is 401 HV_5. Optical microstructure from cross-section of thixo-casts is shown in Fig. 4b. Visible austenite globular grains are surrounded by the eutectic mixture. The insert in Fig.4a shows a histogram of grain size calculated on the basis of the microstructure in Fig 1. The distribution of grain size is within 15μm to 90μm. The largest fraction belongs to the grains in the range of 39 μm to 48 μm, indicating the average size of globules – 44 μm.

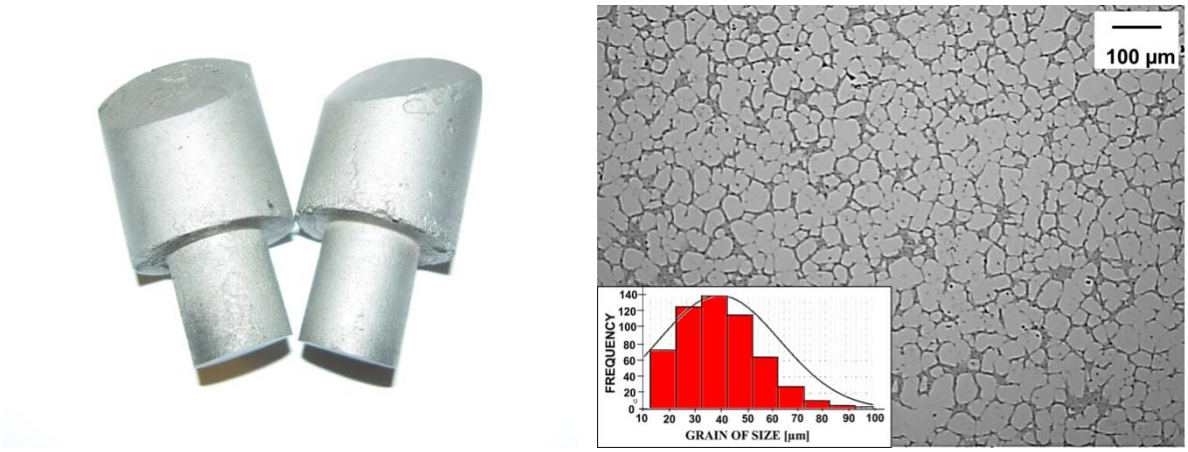

Fig 4 a) Thixo-cast samples of main bucket teeth

b) Microstructure of the main bucket tooth thixo-casts made of steel X210CrW12 and quantitative analysis of grain size distribution

Figure 5 shows SEM microstructure of thixo-casts. Globular grains of solid solution are visible surrounded by the eutectic. Line scan analysis was performed along the marked dotted line along globular grains and the eutectic. Analysis included Fe Kα, C Kα, Cr Kα, W

Kα characteristic spectra. Increased content of Cr and C in the eutectic area indicates high carbides content. Chemical composition of the austenite in globules, as presented in the previous paper [27], was: 2,5% C, 0,4% Si, 0,7% Mn, 8 % Cr, 1,3% W, 0,1%V, 91% Fe and also of the eutectic mixture: 5% C, 0,4% Si, 0,6%, Mn, 17,5% Cr 1,1% W, 75,4% Fe. Quantitative X-Ray analysis (Fig 8a) confirms the presence of 11,8% α-Fe, 82,4% γ-Fe and 5,8% $(Fe,Cr)_7C_3$ carbides [27]. Such a considerable amount of austenite is connected with the increased contents of Cr and C in solid solution stabilizing austenite, and rapid cooling from the solid-liquid range which leads to its stability at room temperature.

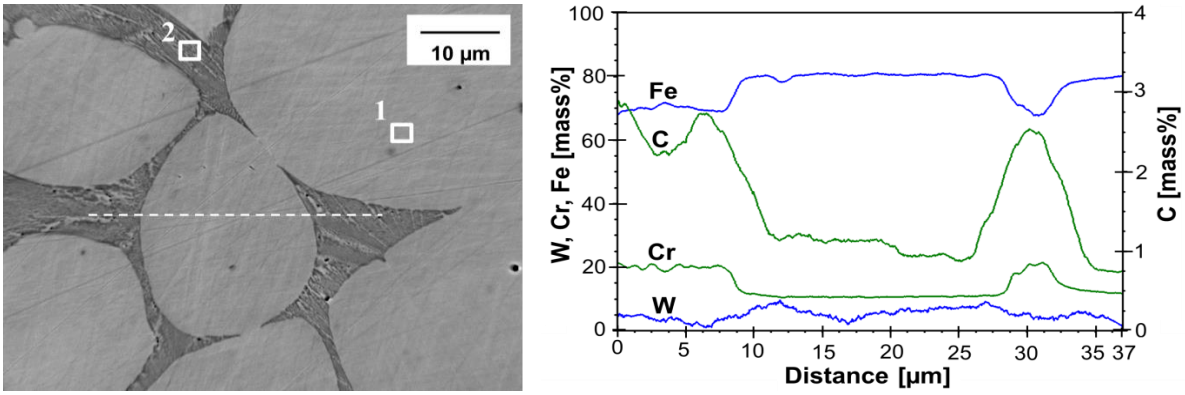

Figure 5 a) SEM micrograph (with line scan composition change of characteristic radiation measurement Fe Kα, C Kα, Cr Kα, W Kα) of X210CrW12 steel after thixoforming

4. LITERATURE

[1] B. Spencer, R. Mehrabian, M. C. Flemings, Metall. Trans. Vol. 3, (1972) 1925

[2] M .C. Flemings, Metall. Trans. A 22A (1991) 957

[3] F. Czerwinski, JOM, Vol.58, Issue: 6, (2006) 17

[4] D. H. Kirkwood, Int. Mater. Rev. 39 (5) (1994) 173

[5] W. Puettgen, W. Bleck, G. Hirt, In. Adv. Eng. Materials, 9 (2007) 23

[6] G. Hirt, R. Kopp, Thixoforming Semi-Solid Metal Procssing. Wiley-vch 2009

[7] F. Czerwinski, Magnesium Injection Molding, Springer, 2008

[8] T. J. Chen, Y. Hao, Y.D Li, Materials and Design Vol.28, Issue 4, (2007) 1279

[9] H. V. Atkinson, in : G. Hirt, A Rassili (Ed), Solid State Phenomena, (2008) 141

[10] R. Kopp, H. Shimahara, J. M. Schneider, D. Kurapov, R. Telle, S. Munstermann, E. Lugscheider, K. Bobzin, Steel Research International,2004, Vol 75,(2004) 569

[11] L. Rogal, in: W. Huang, Y. Kang, X.Yang (Ed.), China Transactions of Nonferrous Metals Society of China, Vol. 20, Elsevier, Science Press, September, (2010) 1033

[12] Z. Fan International Materials Reviews Vol. 47, (2002) 1

[13] H. V Atkinson, A. Rassili, International Journal of Material Forming Vol. 3,(2010) 791.

[14] Li, Jing-Yuan; Sugiyama, Sumio; Yanagimoto, JunJournal of Materials Processing Tech. Vol. 161, (2005) 396

[15] Kopp, Reiner; Kallweit, Jens; Möller, Thorsten; Seidl, Ingold Volume: 130-131, (2002) 562

[16] J. Dutkiewicz, International Journal of Material Forming, Volume 2, (2010) 753

[17] W. Puettgen, W. Bleck, G. Hirt, In: Adv. Eng. Materials, 9 (2007) 231

[18] D. I. Uhlenhaut, J. Kradolfer , W. Puttgen , J.F. Loffler, P.J. Uggowitzer, Acta Materialia 54 (2006) 2727

[19] F. Knauf, I. Seidl, G. Hirt, Solid State Phenomena,Vol. 116-117 (2006) 464.

Acknowledgements

This paper was created within the project "Creation of an international scientific team and incorporation to scientific networks in the area of nanotechnology and unconventional forming material. CZ.1.07/2.3.00/20.0038", which is financed by the European Social Fund and state budget of the Czech Republic.

european social fund in the czech republic
EUROPEAN UNION
MINISTRY OF EDUCATION, YOUTH AND SPORTS
OP Education for Competitiveness
INVESTMENTS IN EDUCATION DEVELOPMENT

Mechanical Characterization of Nanomaterials with the Use of Mini – samples

Jan DŽUGAN [a], Pavel KONOPÍK [a], Radek PROCHÁZKA [a]

[a] *COMTES FHT a.s., Průmyslová 995, 334 41 Dobřany, ČR,*

jan.dzugan@comtesfht.cz

Abstract

A wide range of currently produced bulk nanomaterials are produced by severe plastic deformation (SPD) technologies. Common SPD methods are Equal Channel Angular Pressing (ECAP), High Torsion Pressure (HPT) and Constrain Groove Pressing CGP. Typically, small volumes of nonastructured materials are obtained. Thus if mechanical properties of materials investigated are to be evaluated, special techniques using miniature samples have to be applied. There has been performed extensive attention to development of a Micro Tensile Test (TM-TT) technique for testing of miniature samples. M-TT samples are made of same material volume as in the case of widely used small punch test which is requiring known correlation parameters for the material investigated, while M-TT should be able to assess also unknown materials, as there is carried out the same evaluation as in the case of standard tensile test.

Development of M-TT method is discussed here with special attention to strain measurement that is crucial for accurate tests results. There were employed mechanical extensometer, videoextensometr and also Digital Image Correlation technique for the strain measurement and results of these measurements are compared with standard tests.

Keywords

Nano-material, micro-tensile test, Digital image correlation

1. INTRODUCTION

Materials with nanostructure are of the recent interest and demand for such a kind of materials is gradually increasing. With development of such a kind of materials is closely related demand on description of the material properties as development of these materials is usually carried out on small size samples. Thus for material mechanical properties assessment special testing procedures has to be employed. There has been performed extensive attention to development of a Micro Tensile Test (TM-TT) technique for testing of miniature samples. M-TT samples are made of same material volume as in the case of widely used small punch test which is requiring known correlation parameters for the material investigated, while M-TT should be able to assess also unknown materials, as there is carried out the same evaluation as in the case of standard tensile test.

Development of M-TT method is discussed here with special attention to strain measurement that is crucial for accurate tests results. There were employed mechanical extensometer, videoextensometr and also Digital Image Correlation technique for the strain measurement and results of these measurements are compared with standard tests.

2. MICRO-TENSILE TESTS

The problems with correlation function determination in the case of SPT lead to development of testing procedure for tensile tests, but with the same volume of testing material volume as in the case of SPT where standard sample dimension are 8mm diameter and 0,5mm thickness. Thus samples were designed and appropriate testing fixtures for testing of micro-samples were designed and machined subsequently in order to enable testing. Geometry of proposed sample can be seen in **Fig. 1**. Sample dimensions are following: outer diameter ***D*** is 8mm, thickness ***t*** is 0,5mm, sample active length L_0= 3 mm and active part width a_0 is 1,5mm. Micro-samples were tested in developed fixture shown in **Fig. 2**.

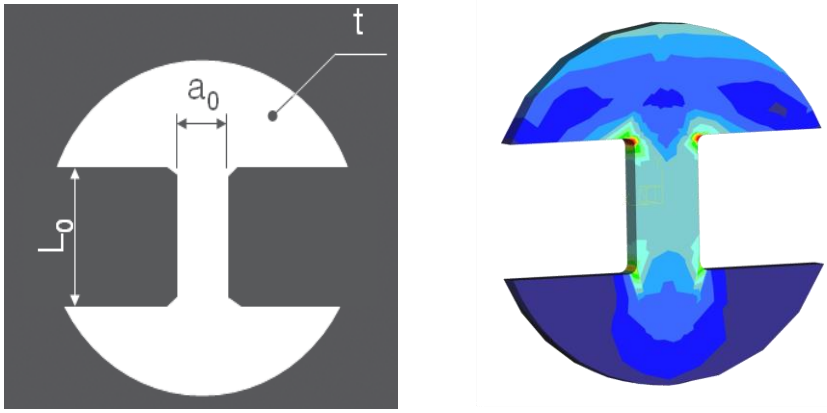

Fig. 1 Micro-tensile sample geometry with stress distribution simulation

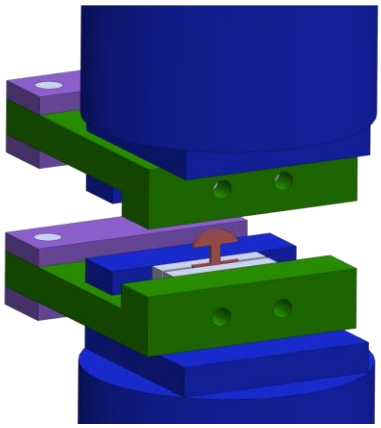

Fig. 2 Testing fixture for micro-tensile samples testing

Tests were executed in servo-hydraulic system with 10kN capacity under strain rates corresponding with CSN EN 100002-1. Elongation and cross section reduction was determined on the basis of sample dimensions after test measurement. Broken samples dimensions measurement was performed with the use of microscope.

In the course of tensile tests is crucial strain measurement and thus a special care was paid to this and three methods were applied: mechanical extensometer, videoextensometer and finally

Digital Image Correlation (DIC) system ARAMIS. There were used different materials for each set of tests, as tests were performed at different times after evaluation of the results from previous step. In all cases there are shown comparisons of M-TT with standard tensile samples for reference.

Mechanical extensometer was used at first. Testing set up can be seen in **Fig. 3**. The extensometer is too big for the considered sample to be attached directly on the sample and thus, it was attached on the testing fixture as close to the sample as possible. Records obtained with this testing set up can be seen in **Fig. 4**.

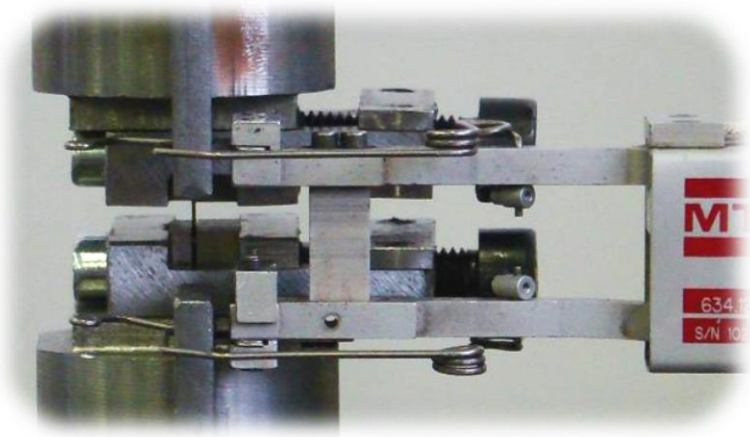

Fig. 3 Testing set up with mechanical extensometer

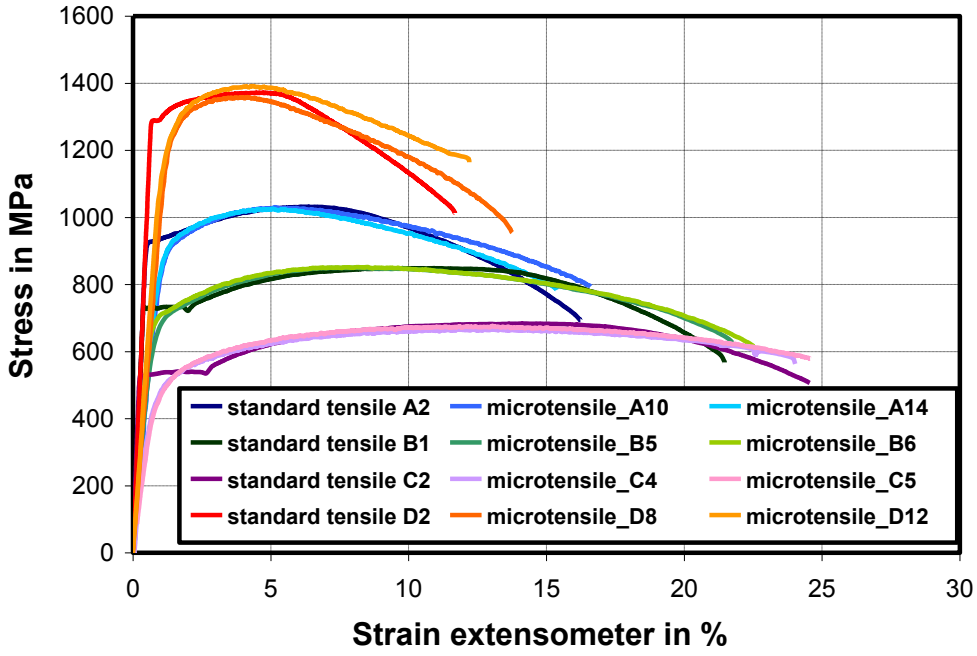

Fig. 4 M-TT records compared with standard tensile tests for mechanical extensometer

As there were some disagreements between standard tensile tests and M-TT in the initial part of the tensile curve where yield stress is evaluated, more accurate strain measurement seems to be necessary and thus videoextensometer measuring the strain directly on the sample was applied. Testing set up can be seen in **Fig. 5**. Course of the test was documented as a video

out of which some pictures documenting the test course are shown in **Fig. 6**. Records obtained with this testing set up can be seen in **Fig. 7**.

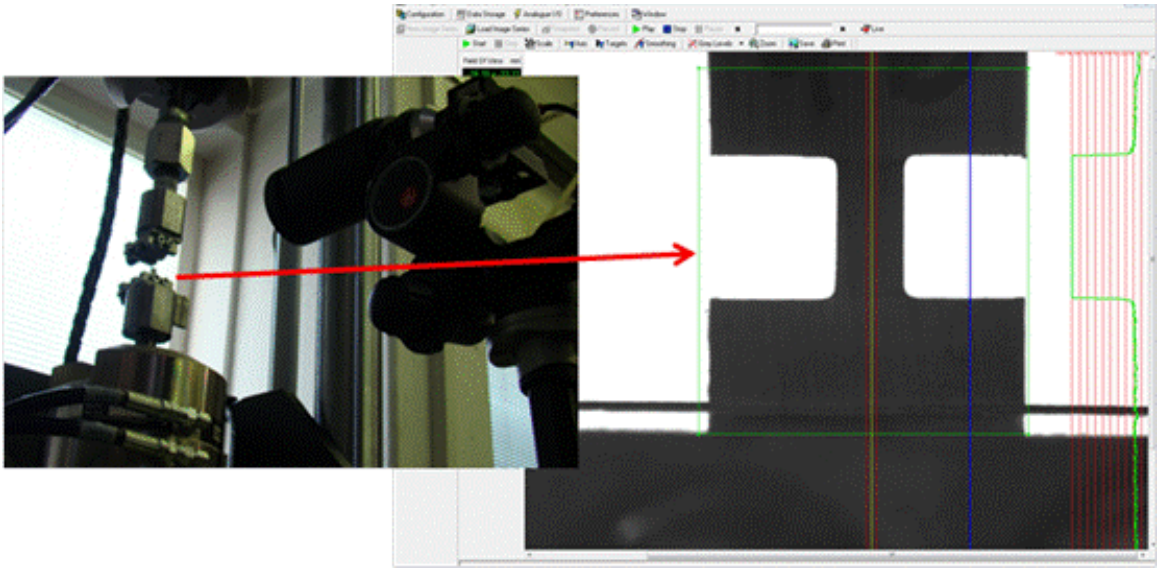

Fig. 5 Testing set up with videoextensometer

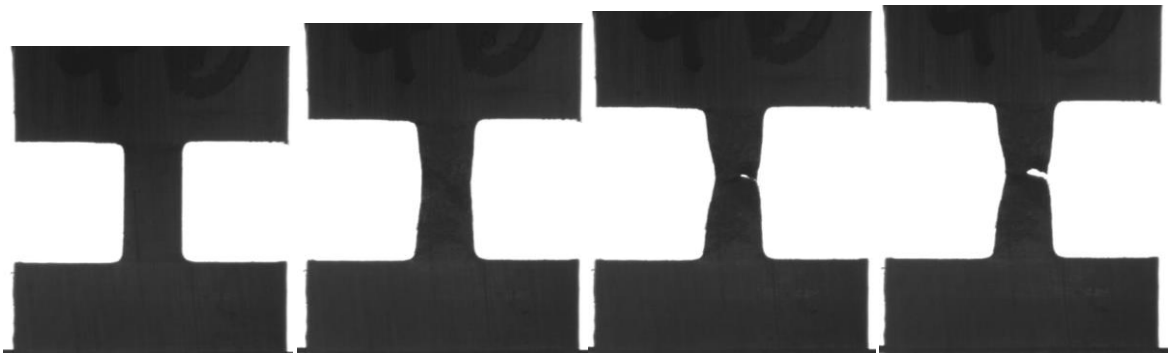

Fig. 6 Images of sample loading in the course of the test with the videoextensometer

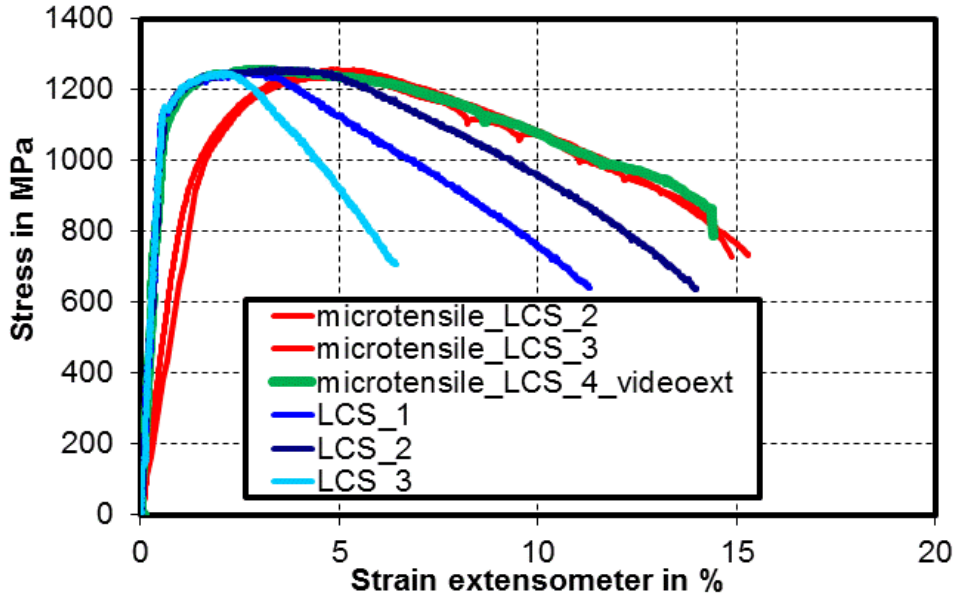

Fig. 7 Examples M-TT records compared with standard tensile tests for videoextensometer

The final step in accurate strain measurement was application of ARAMIS DIC system. Testing set up can be seen in **Fig. 8**. Course of the test with evaluated local strains is shown in **Fig. 9**. Records obtained with this testing set up can be seen in **Fig. 10**.

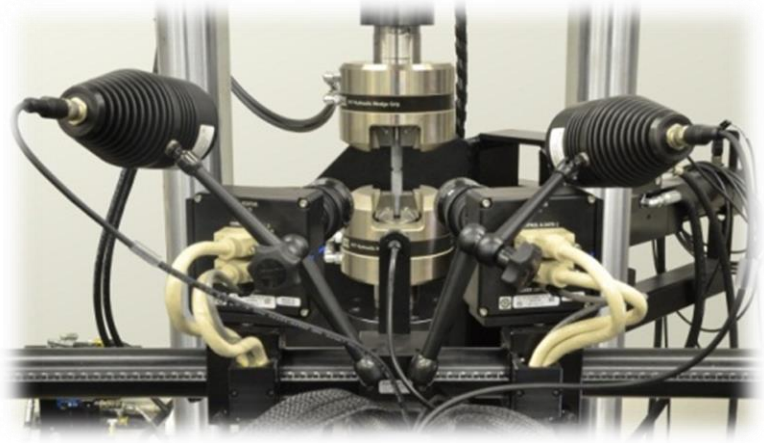

Fig. 8 Testing set up with DIC

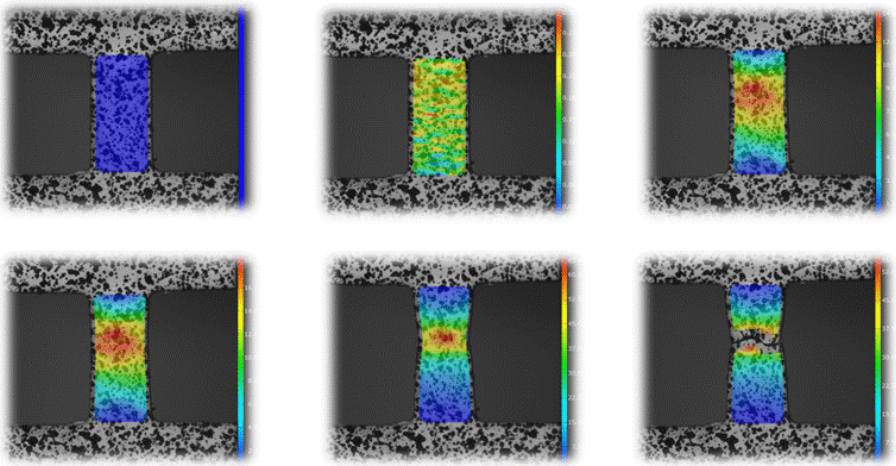

Fig. 9 Images of sample loading in the course of the test with the DIC

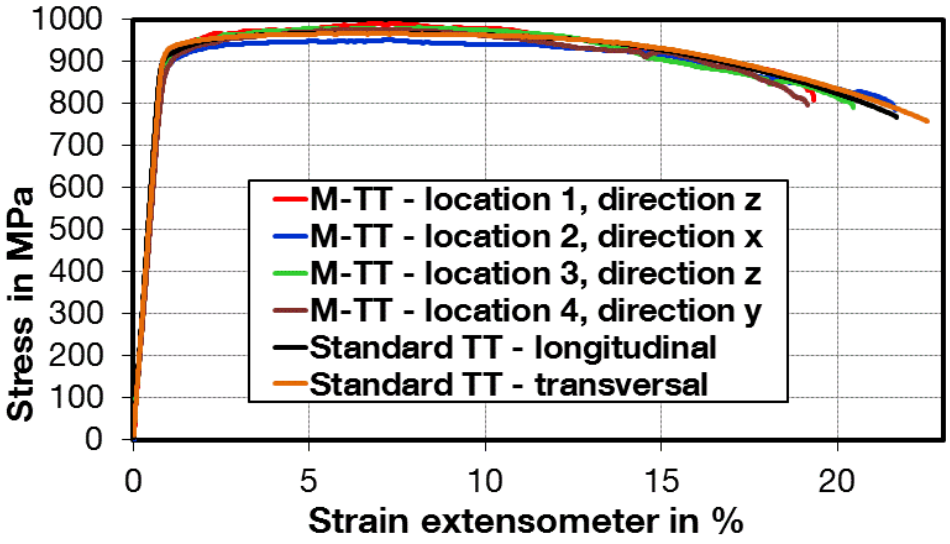

Fig. 10 Examples M-TT records compared with standard tensile tests for DIC

3. RESULTS DISCUSSION

There was proposed M-TT sample geometry and testing fixture. There were performed micro tensile tests with three different testing set ups for strain measurement, as this is a crucial point in the case of tensile test. Mechanical extensometer was applied in the first case and subsequently two optical systems were used later on – videoextensometer and digital image correlation system. Tensile curves obtained from micro tensile samples and standard tests are compared in **Figs. 4, 7** and **10** for each of the applied testing method.

There can be seen slight disagreement with standard tests in the initial part of the tensile curve in the case of mechanical extensometer measurement, **Fig. 4**. This is due to the fact, that the extensometer is attached to the fixture and not directly on the samples as it is in the case of standard tests. This restriction in the case of mechanical extensometers can be hardly overcome, as the mechanical extensometers are bulky and “heavy” for this kind of specimens. Therefore, optical methods for the strain measurements were applied. Both used methods videoextensometer and DIC provided excellent agreement of measured curves with standard tests as can be seen in **Figs 7** and **10**. Almost identical curves are obtained with M-TT samples in comparison to standard ones if these two methods are used.

4. CONCLUSIONS

The paper is dealing with possibilities of mechanical properties evaluation of materials with nano-materials where strongly limited amount of the experimental material is available during the material development. There was investigated testing of micro-tensile testing (M-TT) method in this paper. The results of M-TT were compared with standard tensile tests results here.

As a first step micro tensile test sample geometry was proposed with subsequent design and manufacturing of testing fixture. Accurate results of tensile test are strongly dependent on the strain measurement in the course of the test. There were applied tree methods of strain measurement during M-TT. There was used mechanical extensometer at first that was due to the size restrictions attached to testing fixture. Subsequently, optical methods were applied. Namely videoextensometer and digital image correlation system were used. Measurements with mechanical extensometer provided very good results concerning the tensile strength. Slight problem appeared for yield stress determination, as the initial part of tensile curve was measured with lower accuracy. Optical strain measurements methods provided very good results in comparison with standard tensile tests over whole tensile curves. Both videoextensometer and DIC systems provide efficient and reliable way of strain measurement on M-TT samples and with their use fully comparable results with standard tensile tests can be attained.

The method applicable for tensile properties determination with the use of miniature tensile samples is proposed here. The method is applicable in cases when limited amount of the experimental is available such as testing on bulk nanostructured materials.

Acknowledgements

This paper was created within the project "**Creation of an international scientific team and incorporation to scientific networks in the area of nanotechnology and unconventional forming material. CZ.1.07/2.3.00/20.0038"**, which is financed by the European Social Fund and state budget of the Czech Republic.

european social fund in the czech republic
EUROPEAN UNION
MINISTRY OF EDUCATION, YOUTH AND SPORTS
OP Education for Competitiveness
INVESTMENTS IN EDUCATION DEVELOPMENT

Use of instrumentation of the Department of Materials Technology of the Silesian University of Technology in Katowice at the preparation of joint projects in the field of SPD technologies within the project "Nanoteam VŠB-TU Ostrava"

Eugeniusz HADASIK [a], Dariusz Kuc [a], Lubomir Cizek [b], Stanislav Rusz [b]

[a] *Silesian University of Technology, Faculty of Materials Engineering and Metallurgy, Krasińskiego 8, 40-019 Katowice, Poland*

Eugeniusz.hadasik@polsl.pl, Dariusz.kuc@polsl.pl,

[b] *VSB – Technical university of Ostrava, 17. Listopadu 15, CZ 708 33 Ostrava – Poruba, Czech Republic, lubomir.cizek@vsb.cz, stanislav.rusz@vsb.cz*

Abstract

The report of the European Commission MAG TECH 1 (2004) "Magnesium alloys and processing technologies for lightweight transport applications" refers to the necessity of intensification of research and development works on magnesium alloys and of their subsequent applications, especially in the area of the entire transport.

International collaboration in these areas, especially between universities and research institutes, is of great importance. The Department of Materials Technology of the Silesian University of Technology in Katowice, Poland, in addition to its other activities, collaborates closely with the Department of Mechanical Technology, at the Faculty of Mechanical Engineering of the VSB-TU Ostrava, Czech Republic.

The working site is equipped with the following basic devices:

- Hydraulic press with the max. forming force of 150 t
- Proprietary equipment for the process of forward extrusion
- Chamber furnace CARBOLITE CWF13/13.

Keywords

International co-operation, Silesian University of Technology, Hot pressing process, magnesium alloys

1. INTRODUCTION

Since the beginning of the 21st century we see a recurring significant interest in magnesium alloys and their applications in the automotive and aerospace industries. The automotive industry is interested in them primarily in connection with possible reduction of weight and of fuel consumption. The aerospace industry uses these alloys for the fuselage of aircrafts and for components in the cockpit. New areas of use of Mg alloys are opened to us by new production technologies and their enhancements, such as:

- Processing of new alloys
- New technologies for foundry processes production
- Enhancement of forming technologies with use of the SPD method

Production of new coatings ensuring protection of materials against corrosion

The report of the European Commission MAG TECH 1 (2004) "Magnesium alloys and processing technologies for lightweight transport applications" refers to the necessity of intensification of research and development works on magnesium alloys and of their subsequent applications, especially in the area of the entire transport.

The following is expected to bring:

- Development of foundry technologies
- Intensive development of forming technologies

International collaboration in these areas, especially between universities and research institutes, is of great importance. The Department of Materials Technology of the Silesian University of Technology in Katowice, Poland, in addition to its other activities, collaborates closely with the Department of Mechanical Technology, at the Faculty of Mechanical Engineering of the VSB-TU Ostrava, Czech Republic.

The working site is equipped with the following basic devices:

- Hydraulic press with the max. forming force of 150 t
- Proprietary equipment for the process of forward extrusion
- Chamber furnace CARBOLITE CWF13/13.

2. PROCESSES OF EXTRUSION OF MAGNESIUM ALLOYS

Extrusion is a plastic treatment process in which with the use of piston rod or punch (usually through blowing egg) a pressure is exerted on the material placed in a container (called recipient) forcing the material to flow out though the die cavity or the slot between the punch and the walls of the recipient (fig.1). Initially, due to very intensive pressing, extrusion was used mainly to shape the products from materials characterised with low yield point such as: Pb, SN, Al, Cu and their alloys. Due to the development of extrusion technologies, as a result of application of heating the charging material and tools as well as application of special lubricants (with high ignition temperature), it was possible to extrude steel and other metals with high melting temperature. Wide application possibilities and popularisation of the process occurred when aluminium and its alloys were applied in aviation and machine industries. Extrusion of those materials proceeds at a small speed of tools and in low temperatures. At present, with the growth in popularity of magnesium alloys extrusion is a process which is commonly applied also in their processing.

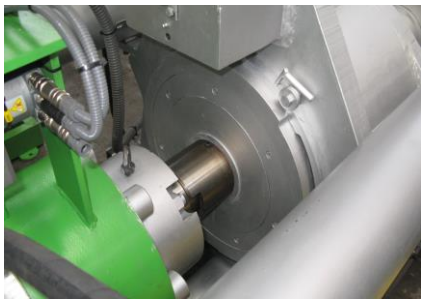

a) view of the recipient with charging material

b) extruded rod

Fig. 1 Press PHP – LR500

Simple technology provides small material losses and relatively low costs of manufacturing. Taking into account the temperature of the charging material the extrusion process can be divided into:

- **cold extrusion –** applied for extrusion of products which are expected to have extended mechanical properties, high precision of dimensions and size, smoothness of surface and proper structure;
- **heat extrusion -** in this process elevation of temperature allows for achievement of products with slightly worse quality of surface and accuracy of stampings. However, bigger plasticity of metal and as a result smaller force of extrusion enables to conduct the plastic treatment process with application of significantly bigger strains;
- **hot extrusion –** is usually applied for extrusion of rod, pipes and sections, which are, in the next stages, undergoing processes of finishing treatment. Products achieved in this are characterised with worse mechanical properties, worse surface quality and more defects (i.e. crackings).

Among special methods of extrusion there are:

- hydrostatic methods
- Conform
- KOBO
- continuous casting

3. RESEARCH POST AT SILESIAN UNIVERSITY OF TECHNOLOGY

Tests conducted within this report aimed at formulation of the basis for technology of hot forward extrusion process of magnesium alloy AZ31. Tests were conducted on research post in Department of Materials Technology at Silesian University of Technology. The post consists of the following elements:

- Vertical hydraulic press with maximum compression force 150 tonnes (fig. 2a) with a device constructed individually to conduct process of forward extrusion (fig. 2b). Press is equipped with computer steering system (fig. 3) which allows for regulation of parameters of functioning of a device and fully automated conduction of tests. This system also allows for registration of the basic parameters during conducted tests.

- Prototype press KOBO with compression force up to 250 tonnes (fig. 4)

- Chamber furnace CARBOLITE CWF13/13 (fig. 5)

a) Unit device

b) Detail to conduct process of forward extrusion

Fig. 2 Vertical hydraulic press with maximum compression force of 1500kN

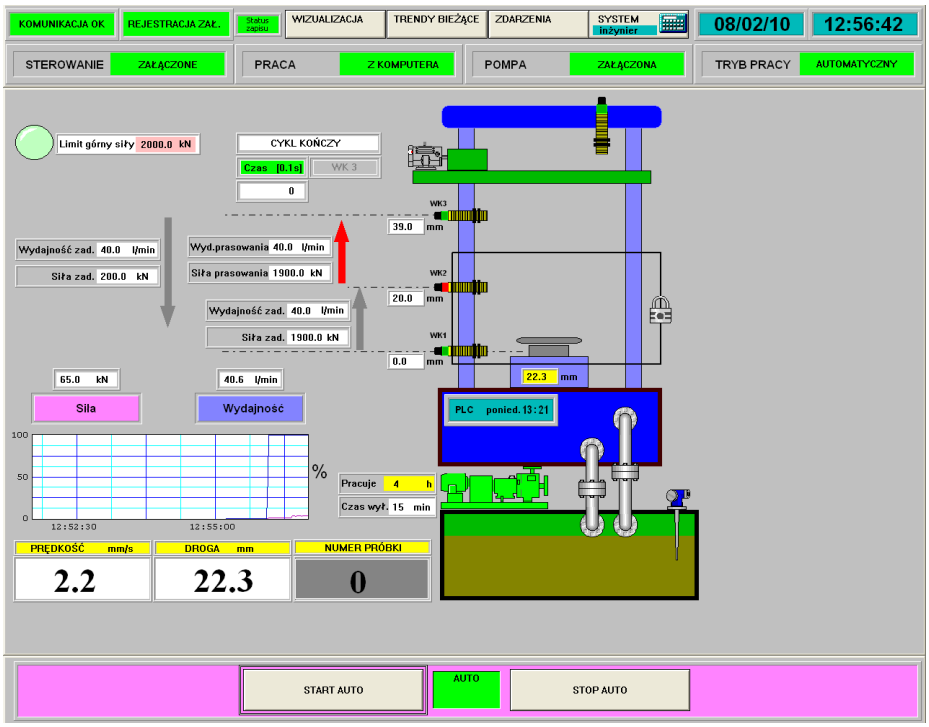

Fig. 3 Window of computer program for steering and registration of parameters of vertical hydraulic press with compression force of 1500kN

Hydraulic press presented in fig. 2a is a two-column press working vertically. Maximum compression force for this press is 1500kN, but its construction may allow reaching a maximum force of 2000kN. Due to application of two leading columns the press is characterised with big working space which allows for its application in conduction of tests for various processes of plastic treatment, such as extrusion, forging or stamping. Conduction of the process of forward extrusion on hydraulic press was possible due to application of special equipment. Construction of the device for extrusion allowed for extrusion of products from ingot with a diameter of 40mm. Thanks to possibility of application of various dies the device allows for production of rods with different diameters. At present there are dies applied which allow for production of round rods with dimensions of 14, 12 and 10mm. Preparation of device from steel to be able to hot process the material allowed to heat the recipient to the temperature of the ingot.

In recent years the KOBO method has become very popular (fig. 4). The name of the method comes from first letters of the names of its inventors: Korbel and Bochniak. In this method, besides the traditional system with which the material can be axially pressed, a reverse movement of die is added which uses torsion with the right angle and the right frequency and makes the process of extrusion easier.

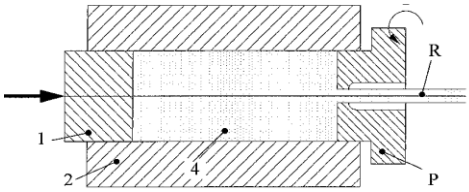

1-punch, 2-recipient, 4- extruded material,

P- two-sided rotation die, R- product

a) Diagram of extrusion with the use of KOBO method

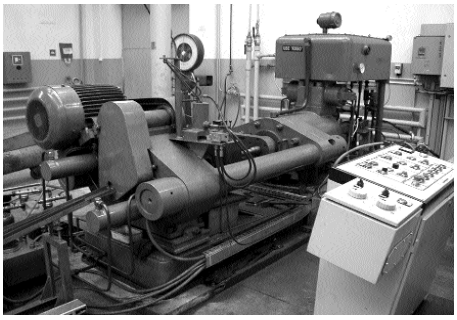

b) cell view

Fig. 4 Prototype KOBO press

Chamber furnace CARBOLITE CWF13/13 (fig. 5) can be used to heat both the extruded ingot and the whole device to the wanted temperature of the process. It is possible due to heating chamber with dimensions of 200×200×325mm. Maximum temperature of furnace at work is 1300°C. Applied PID regulator for steering allows inter alia to conduct heating process with regulated speed, to set heating temperature precisely and to performed regulated cooling.

Fig. 5 Laboratory chamber furnace CWF13/1

4. LABORATORY TESTS OF THE EXTRUSION PROCESS OF MAGNESIUM ALLOY AZ31

On the basis of literature data analysis it was stated that the process of extrusion of alloy AZ31 can be conducted in temperature range 200÷400°C. The dimensions of the ingot were adjusted to the dimensions of recipient.

Testing material was rod with ϕ 12 mm from magnesium alloy AZ31, achieved in the process of hot extrusion from charging material with ϕ 30 mm;

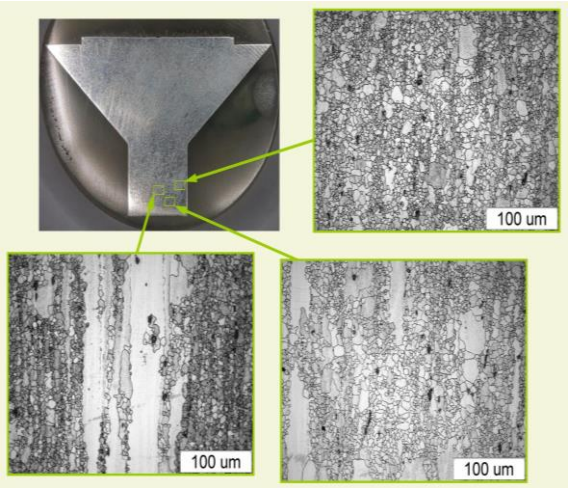

Fig. 6 Microstructure of alloy AZ31 after extrusion process for ϕ12 mm.

5. SUMMARY

International collaboration in these areas, especially between universities and research institutes, is of great importance. The Department of Materials Technology of the Silesian University of Technology in Katowice, Poland, in addition to its other activities, collaborates closely with the Department of Mechanical Technology, at the Faculty of Mechanical Engineering of the VSB-TU Ostrava, Czech Republic.

The paper is devoted to analysis of the influence of extrusion process on the microstructure and properties of magnesium alloys AZ31. Tested alloy in initial state has heterogeneous, coarse-grained structure. After extrusion process no cracking were found on the surfaces of the rods with diameters 20 and 36mm and tests of microstructure show grain refining which is the biggest in the sub-surface area of extruded rods. Such significant grain refining results from the occurrence of dynamic recrystallisation in temperature of extrusion. It was stated, on the basis of measurements of micro-hardness that there is a significant diversification of hardness depending on the diameter of the rods which proves the heterogeneity of the deformation.

Acknowledgements

This paper was created within the project "**Creation of an international scientific team and incorporation to scientific networks in the area of nanotechnology and unconventional forming material. CZ.1.07/2.3.00/20.0038"**, which is financed by the European Social Fund and state budget of the Czech Republic with cooperation of the Silesian University of Technology Katowice (support of Structural Funds in the Operational Programme - Innovative Economy (IE OP) financed from the European Regional Development Fund - Project "Modern material technologies in aerospace industry", Nr POIG.01.01.02-00-015/08-00)

INVESTMENTS IN EDUCATION DEVELOPMENT

Using of nanomaterial at industrial experience

Marcel KLOS[a],

[a] *VSB – Technical university of Ostrava, 17. Listopadu 15, 708 33 Ostrava – Poruba, CZ, E - mail: mklos@visteon.com*

1. INTRODUCTION

The develop aspects automotive industries repose in the time new on used materials.

Company which are in Czech Republic Global producer of air condition system of the care and other company is connected material producer. Customers of these companies are Global care producer for example Ford, Mercedes, PSA, Fiat, Bentley.

Companies occurring in automotive industries represented by these branches industries have new requirements on materials in term of high corrosive immunity, stability of size, increasing formability and high mechanical properties.

In individuals requirement is increasing pressure on changes of conventional material for example steel and stainless steel for used as material connection two components. In time is an existing new requirement for material on base aluminium and titanium.

Global automotive industry given of emphasis on decreasing total price of components in the last three years. An imported factor for global care producer is minimal price of used components. These reasons are imported factors for applications nano-materials in serial productions.

The employment in automotive production among leaders USA, Japanese and EU. Automotive industry in EU is major employer (43%). In years 2010 and 2011 was potential growth in automotive industry on same value as year 2006-2007, but by increasing productivity of production about 15%-20%. [6,12]

2. LEADERS EMPLOYMENT PRODUCTIVITY

Improving of product quality in automotive industries and efficiency of methodology in production is the most important for automakers invest a large amount of time and money into developing and improving the global manufacturing process at the market, and rely heavily on research and technological innovation – materials, tools, machine. After global crises the last years, significant technological development has taken place, changing and reinventing „how vehicles are produced and how should by leaders employment productivity“.

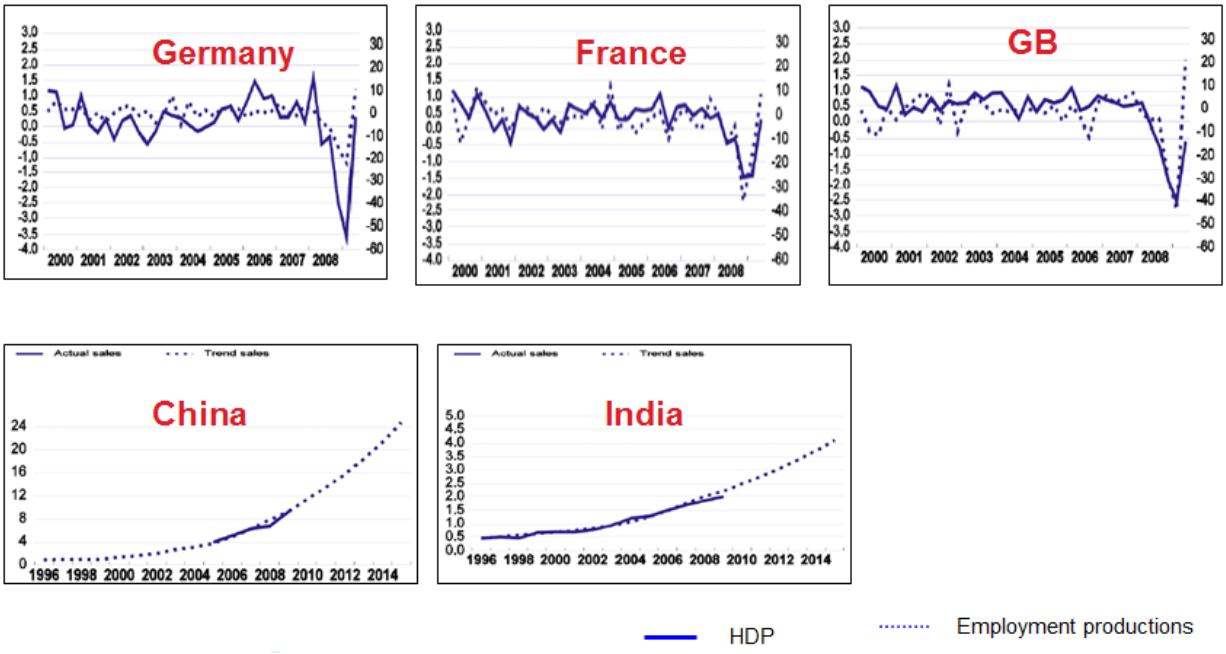

Fig. 1 Employment and economic productivity in the face of HDP (Employment/HDP) [1]

Productivity in Czech Republic is about 30-40% and productivity is approximately between 50-60%. Global Productivity in market and production in EU is about 85 %. The companies over the 75 years building of optimal leadership for staff. [6]

In physiological are all other motivations become secondary. The main factors are satisfied and next motivational is higher productivity of products. For employees which working on routine jobs have be tendency anti motivate point of view social and psychological.

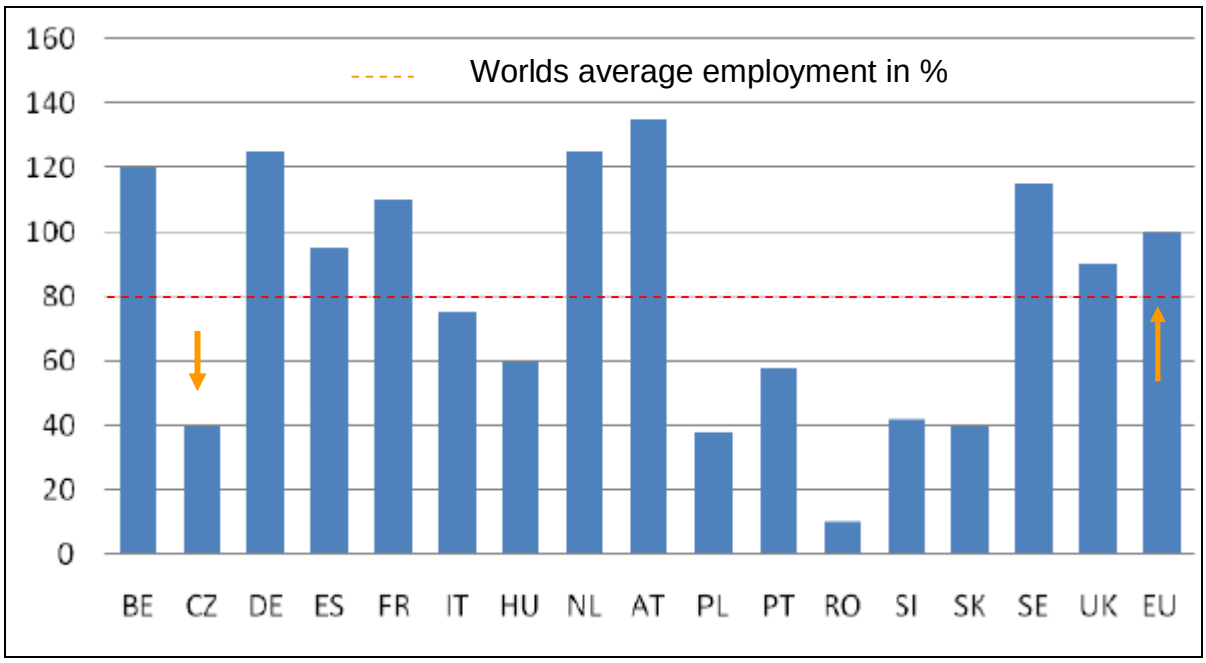

Fig. 2 Productivity EU [4,8]

Automation will the automotive industry be able to effectively reduce costs and therefore survive in an international. The main factor to higher productivity, efficiency, and complete global quality is important of implementation new vision systems and materials.

In automobile manufacturers is guarantee make of assembly and processing 24 hours, 7 days per week. They potential factors are for economic efficiency in automotive industrial and effective solutions for complex tasks of manufacturing and global market.

3. AUTOMOTIVE INDUSTRY - STRATEGY

Developed activity should by coasted maximal 13% with product total price. Every year is development pressure on the total cost about 3% with total price. Typical Develop time – Maximal time is 2 years, Maximal time for component implemented in serial production a 6-8 years.

The proposals to make automotive industrial more competitive by investing in innovation, transformation or close red branches division in company. Keeping the automotive industry is important for Europe's prosperity. Meeting these challenges means companies need to focus more on quality and innovation. Carmakers are under pressure from developing of global customers and countries in which is small production and higher demand of new cares.

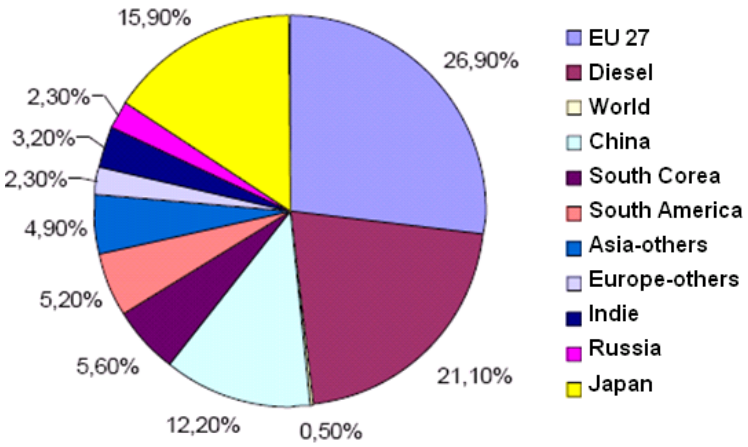

Fig. 3 Global vehicle productivity [2]

4. NANOMATERIAL'S IMPLEMENTATION IN AUTOMOTIVE INDUSTRY

Recent developments aluminum alloy on base UFG (standard alloy: 3xxx, 5xxx, 6xxx, 8xxx) and processes have influence of improved the creep and corrosion resistance, mechanical properties. The results conclude that reasonable prices and improved properties of alloys will lead to massive implementation to construction of vehicles. Compared to using alternative materials (UFG) and using of standard alloys lead to higher of results (mechanical properties) about in a 20-25%. Lastly, the use of

UFG material in automotive as composites.

Nanomaterial's could be implemented in serial production as connection material:

- Components in the engine, holders
- Component for undercarriages prevention (tube, plate)

Automotive have special ***requirements on mechanical properties*** ↑ ***&*** ***Total price*** ↓

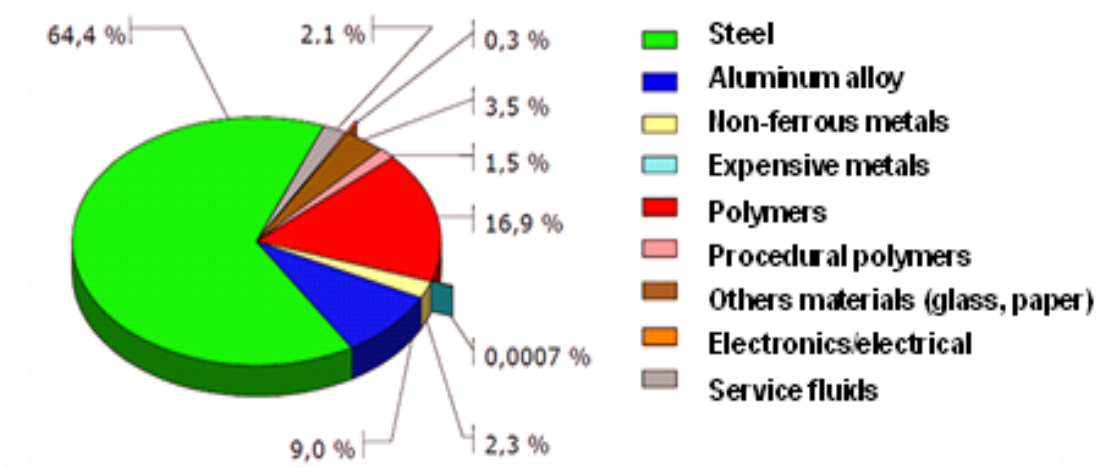

Fig. 4 Materials in automotive industry [1,8,7]

5. CONCLUSIONS

The objective is the applications of materials on base UFG in the automotive industry that can significantly contribute to greater fuel economy and environmental innovation. The nanomaterial's usage of in automotive applications can be taken as benefits for strong strategy. Strategy of automotive industry in Czech Republic is per 70% manufacturing only. Nanomaterial's could be used as join venture between economical subject (connection materials (bold), engine components, holders). Principle of automotive industry is develop pressure on suppliers – task is price decreasing about 3% every year. European and USA vehicle markets are very insufficiency for nonmaterial's. Important vehicle market for develop is China and India.

6. LITERATURE

[1] Automotive Aluminum [.online]. c2006 [.cit. 2008-05-20]. Dostupný z WWW: <http://www.autoaluminum.org>.

[2] BMW Group PressClub [.online]. 2000-2009 [.cit. 2009-02-05]. Dostupný z WWW: <http://www.press.bmwgroup.com>.

[3] BMW X5 Fender : Case Study. [.s.l.] : [.s.n.], c2007. Dostupný z WWW:

<http://www.borealisgroup.com/pdf/literature/borealis/casestudy/K_CAST048_GB_AA_2007_10_B.pdf>. s. 1-2.

[4] BOUCNÍK, P., ČECH, J., JUŘIČKA, I.: Použití hořčíkových slitin ve slévárenství. 5. Medzinárodna vedecká konferencia CO-MAT-TECH, Trnava, 14.10. - 15.10.1997.

[5] DAWSON, Steve. Compacted Graphite Iron: Mechanical and Physical Properties for Engine Design. Dresden, 1999. 22 s. Oborová práce. Dostupný z WWW: <http://www.sintercast.com/data/content/DOCUMENTS/200431723285110vdi_paper.pdf>.

[6] GermanCarFans.com [.online]. c2009 [.cit. 2009-05-23]. Dostupný z WWW:

<http://www.germancarfans.com>.

[7] GREGER, Miroslav, et al. Využití hořčíkových slitin v automobilovém průmyslu. In METAL 2008. Hradec nad Moravicí: [.s.n.], 2008. s. 1-12.

[8] HERMAN, Aleš, STUNOVÁ, Barbora. Výhody použití Mg slitin v porovnání s ostatními konstrukčními materiály. MM Průmyslové spektrum. 2005, č. 10, s. 92.

[9] HIRSCH, J.. Automotive Trends in Aluminum, The European Perspective [.online]. Bonn : c2009 [.cit. 2009-05-25]. Dostupný z WWW: <http://www.keytometals.com/Article135.htm>.

[10] HLUCHÝ, Miroslav, KOLOUCH, Jan. Strojírenská technologie : Nauka o materiálu. Praha : Scientia, 2002. 266 s.

[11] JANČÁŘ, Josef. Úvod do materiálového inženýrství kompozitů. Brno : [.s.n.], 1999. 39 s.

[12] Modern Casting.: Magazine for Foundries and Diecasters : Iron Alloys [.online]. c2009 [.cit. 2009-05-21]. Dostupný z WWW: <http://www.moderncasting.com/content/view/629/183/>.

Acknowledgements

This paper was created within the project "**Creation of an international scientific team and incorporation to scientific networks in the area of nanotechnology and unconventional forming material. CZ.1.07/2.3.00/20.0038"**, which is financed by the European Social Fund and state budget of the Czech Republic.

european social fund in the czech republic
EUROPEAN UNION
MINISTRY OF EDUCATION, YOUTH AND SPORTS
OP Education for Competitiveness
INVESTMENTS IN EDUCATION DEVELOPMENT

Mechanical properties of UFG magnesium alloys

Pavel LUKÁČ, Zuzanka TROJANOVÁ

[a] *Charles University in Prague, Fauculty of Mathematics and Physics, Ke Karlovu 5. CZ 121 16 Praha 2, Czech Republic,*

lukac@met.mff.cuni.cz; ztrojan@met.mff.cuni.cz

Abstract

Severe plastic deformation (SPD) technique may produce an ultrafine grained (UFG) microstructure of metallic materials, which leads to a significant improvement of the materials. The results of investigations show that grain refinement is also of significance for magnesium alloys to obtain enhanced properties. Magnesium alloys prepared by equal angel channel processing (ECAP) were deformed at various temperatures. It has been found that reducing grain size leads to a large increase in the strength of ultrafine grained magnesium alloys deformed at room temperature in comparison to that of coarse grained ones. The strength of ultrafine grained magnesium alloys decreases rapidly with increasing test temperature. At higher temperatures the strength of ultrafine grained magnesium alloys may be lower than that of coarse grained ones. On the other hand, the overall ductility prior to failure of ultrafine grained magnesium alloys deformed at room temperature is higher than that of coarse grained ones. The ductility of ultrafine grained Mg alloys increases with increasing test temperature. In some cases, the superplastic deformation behaviour may be observed. It should be noted that the processing route of ECAP is one parameter that can effectively influence the mechanical properties of materials. The mechanical properties can be influenced by the number of passes during ECAP.

Keywords

SPD; grain refinement; mechanical properties; magnesium alloys.

1. INTRODUCTION

Magnesium alloys – as the lightest structural metallic materials – exhibit high specific strength and high specific elastic modulus. Solid solution hardening, precipitation and dispersion strengthening increase the yield strength. A finer grain size may contribute significantly to the strength. The grain size dependence of the yield stress, σ_y, (and also the flow stress and tensile strength) can be expressed by the Hall-Petch relationship in the following form

$$\sigma_y = \sigma_0 + K_y d^{-1/2} \quad (1)$$

Here d is the average grain diameter, σ0 is a constant and Ky – called also the slope of the Hall-Petch relationship – is the stress intensity factor for plastic yielding. It is considered that σ0 is proportional to the critical resolved shear stress (CRSS) for basal slip of a single crystal of the

alloy and Ky is proportional to the square root of the CRSS for the non-basal slip of a single crystal of the alloy. In contrary to FCC alloys where the CRSSes for the primary and secondary slip systems have the same value, the CRSS for non-basal slip systems are higher than that for basal slip system. This may be the reason why the slope of the Hall-Petch relationship for Mg alloys is higher than that for Al alloys. Naturally, the value of Ky depends on the chemical composition of the alloy, its fabrication and the deformation temperature.

Experimental results show that grain size – as a main microstructural factor – influences the physical and mechanical properties of polycrystalline metallic materials. Corrosion resistance – an important property for applications – may be also affected by the grain size.

2. TECHNIQUES FOR GRAIN REFINEMENT

Various techniques are used for the preparation of magnesium alloys with fine grains. Rapid solidification (RS) methods and powder metallurgy (PM) techniques produce a very small grain size. Magnesium alloys processed by a rapid solidification method, in some cases followed by pulverization are consolidated by vacuum hot pressing and extrusion, forging or rolling [1 – 4]. A powder metallurgy method applied to Mg alloys produces a smaller grain size compared to an ingot metallurgy method. Magnesium alloys with very small grain sizes can be also prepared by mechanical alloying [5].

Among the methods used for grain refinement, severe plastic deformation (SPD) techniques produce samples with ultrafine grains. Over the last decades, many papers describing the extreme grain refinement using these SPD techniques have been published. In this work, it is impossible to describe all variants of SPD techniques used for grain refinement. The basic processes used are Equal-channel angular pressing (ECAP), High-pressure torsion (HPT) and Accumulative roll bonding (ARB). Twist extrusion (TE) and Multi-directional forging (MDF) are also oft used.

It should be mention that the total strain of sample introduced by one pass in ECAP (if the angle between the channels is 90°) is about 1 (i.e. 100%). Different routes in ECAP may produce texture.

Only small samples (about 1 mm in thickness can be fabricated by HPT techniques. On the other hand, the grain size may be very small. However, deformation depends on the distance from the sample centre. The shear strain increases from the rotation axis in the radial direction. Deformation is not uniform.

In contrast to rolling, ARB technique produces not-equiaxed grains. A large strain may be produced by repeating rolling.

In contrast to RS and PM technique, the advantage of the SPD methods is the production of materials without porosity. Both types of techniques have a great potential for grain refinement and therefore for enhanced mechanical properties – strength and ductility of a material.

In the case of magnesium alloys, some additions of impurity and minor elements as Fe, Si, Ca, Sr, rare earths (RE) can be a significant grain refiner. These impurity and minor elements act as nucleant particles. Ultrasonic treatment may also cause grain refinement, which depends primarily on the amplitude of the ultrasonic waves [6]. Very recently, a review of models of grain refinement during SPD straining based on the dislocation density has been reported by Estrin and Vinogradov [7].

Substantial features of SPD processing are the following: High strains without failure can be achieved. There is no significant change in the dimensions of the piece. Multi passes operations are possible. Deformation takes place under an extensive hydrostatic pressure. Alloys with ultrafine grains and a high dislocation density are produced. Enhancement of strength is a result of processing; in some cases also enhancement of ductility. It is important to mention that thermal stability, thermal and electrical conductivity may be influenced by SPD processing.

3. STRENGTH OF UFG MAGNESIUM ALLOYS PRODUCED BY SPD

In this chapter we would like to give some examples of the parameters of the Hall-Petch equation (1). It is interesting to note the results obtained very recently by Cáceres et al. [8]. They deformed cast specimens of Mg and some Mg-Zn alloys with a wide range of grain sizes. They estimated the yield strength and the parameters σ_0 and K_y. For pure Mg with grain size d between 19 and 1440 μm, σ_0 = 11.8 MPa and K_y = 0.22 MPa·m$^{1/2}$. The σ_0 and K_y values for the different Mg-Zn alloys are the following: for Mg-0.4Zn with d between 30 and 245 μm, σ_0 = 2.7 MPa, K_y = 0.37 MPa·m$^{1/2}$; for Mg-0.8Zn with d between 25 and 375 μm, σ_0 = 9.1 MPa, K_y = 0.42 MPa·m$^{1/2}$; for Mg-2.3Zn with d between 46 and 500 μm, σ_0 = 7.7 MPa, K_y = 0.65 MPa·m$^{1/2}$. These values were estimated for tension deformation. Caceres et al. [8] estimated the values also for samples deformed in compression. It is clear that the intensity factor K_y increases with the concentration of Zn. It seems the values of K_y obtained in compression are larger.

As mention above, Nussbaum et al. [1] investigated the Hall-Petch relationship for specimens of AZ91 prepared by RS, consolidation and extrusion with d between 5 mm and 0.3 μm. They estimated σ_0 = 130 MPa and $K_{ý}$ = 0.21 MPa·m$^{1/2}$. In the last decades, the deformation behaviour of magnesium alloy AZ31 prepared by SPD has been intensively studied. In the following paragraph we would like present some experimental results concerning to the effect of grain size on the yield strength.

Chino et al. [9] investigated the influence of grain size on the strength for AZ31 simple rolled samples deformed at room temperature. They tested the Hall-Petch equation for the yield stress and showed that σ_0 = 131 MPa and K_y = 0.25 MPa·m$^{1/2}$ for samples with d between 21.5 and 5.2 μm.

Guo et al. [10] studied the effect of grain size on mechanical properties and work hardening behaviour of AZ31 magnesium alloys. Rolled sheets were obtained by flat rolling by 13 passes; the rolled sheets were heated at 773 K for 1 h before final pass. The total rolling reduction was 90%. The effect of grain size on the yield stress was investigated for samples with d between 24 and 7.6 μm deformed at room temperature. The parameters of the Hall-Petsch relation have the following values: σ_0 = 85 MPa and K_y = 0.20 MPa·m$^{1/2}$. For samples with a grain size of 24 μm, σ_0 = 115 MPa and an elongation to fracture of 18% were attained whereas for samples with a grain size of 7.6 μm, σ_0 = 180 MPa and an elongation to fracture of 22% were obtained.

Yoshida et al. [11] concerted on mechanical properties of AZ31 alloy subjected to ECAP. Before ECAP samples were extrude. The relation between grain size and the yield strength was investigated using samples subjected to 8 passes in ECAP and then isochronal annealed at 448-673 K for 1 h and at 673-773 K for 4 h. The obtained samples have grain size d between 32 and 4.5 μm. The variation of the yield strength with grain size can be expressed by the Hall-Petch equation with σ_0 = 30 MPa and K_y = 0.17 MPa·m$^{1/2}$.

Very interesting results have been very recently obtained by Razavi et al.[12]. They investigated the effect of grain size on the yield strength for prismatic slip in AZ31 alloy. The samples were

prepared using multi-temperature ECAP with combination of routes and passes. Twinning was supressed. For details see the reference [12]. The crystallographic texture – strong basal texture – was kept the same, which makes prismatic slip possible. Samples with grain size between 33 μm and 360 nm. The Hall-Petch relationship with two slopes was estimated. For d between 33 and 2.9 μm, σ_0 = 124 MPa and K_y = 0.20 MPa·$m^{1/2}$, whereas for d between 2.9 μm and 360 nm, σ_0 = 208 MPa and K_y = 0.09 MPa·$m^{1/2}$.

As shown by Wang et al. [13], the strain rate sensitivity may be influenced by grain size. They have reported that the strain rate sensitivity of rolled Mg-3Al-3Sn alloy increases with decreasing grain size if the samples are deformed at room temperature. This result indicates a change in the deformation mechanism – in samples with small grains the dislocation glide is dominant whereas in samples with larger size grains twinning is also active.

It is well known that samples with small grains bellow about 10 μm may exhibit superplasticity at elevated temperatures. Watanabe et al. [14] have reported that magnesium alloy ZK61 with a grain size of 650 nm exhibits the superplastic behaviour – if samples were deformed at 473 K at a strain rate of 10^{-3} s^{-1} a large elongation to fracture of 660% was attained. A very large elongation to fracture of 1274% was attained in magnesium alloy WE43 if deformed at 673 K and at a strain rate of $2x10^{-3}$ s^{-1} [15]. The mean grain size of the hot-extruded WE43 alloy samples was 1.5 μm. The strength of fine-grained magnesium alloys decreases with increasing temperature. Then significant problems may occur in application at elevated temperatures when fine grains can grow.

4. CONCLUSIONS

In the literature one can find the value of σ_0 between 10 and 130 MPa and K_y between 0.17 and 0.65 MPa·$m^{1/2}$. The values of σ_9 and K_y depend not only on grain size. The values are influenced by processing methods. Samples may have different dislocation density (affected for instance by the testing temperature or annealing treatment). Samples prepared by SPD may have different textures. Chemical composition due to strengthening mechanisms influences the yield strength and hence the Hall-Petch relationship. Solid solution hardening, precipitation strengthening, and dispersion strengthening should be taken into account. The stable dispersoids are not only obstacles to dislocation movement but also serve as pinning point for grain sliding and grain boundary motion. The severe plastic deformation techniques used in preparation of the material and the heat treatment influence the deformation behaviour of the material – its strength and ductility.

5. LITERATURE

[1] H. Jones: Key Eng. Mater. 97-98, 1994, 1-7.

[2] G. N. Nussbaum, P. Sainfort, G. Regazzoni, H. Gjestland: Scripta Metall. 23, 1989, 1079-1084.

[3] J. K. Solberg, J. Torklep, O. Bauger, H. Gjestland: Mater. Sci. Eng. A 134, 1201-1203.

[4] A. Kato, H. Horikiri, A. Inoue, T. Masumoto: Mater. Sci. Eng. A 179/180, 1994, 707-711.

[5] Z. Trojanová, P. Lukáč, H. Ferkel, B. L. Mordike, W. Riehemann: Mater. Sci. Eng. A 234-236, 1997, 798-801.

[6] M. Quian, D. H. StJohn: Int. J. Cast Met. Res. 22, 2009, 256-259.

[7] Y. Estrin, A. Vinogradov: Acta Mater. 61, 2013, 782-817.

[8] C. H. Caceres, G.E. Mann, J. R. Griffiths: Metall. Mater. Trans. A 42A, 2011, 1950-1959.

[9] Y. Chino, M. Mabuchi, R. Kistira, H. Hosokawa et al.: Mater. Trans. 43, 2002, 2554-2560.

[10] L. Guo, Z. Chen, L. Gao: Mater. Sci. Eng. A 528, 2011, 8537-8545.

[11] Y. Yoshida, L. Cisar, S. kamado, Y. Kojima: Mater. Trans. 44, 2003, 468-475.

[12] S. M. Razavi, D.C. Foley, L. Karnan, K.T. Hartwig et al.: Scripta Mater. 67, 2012, 439-442.

[13] H. Y. Wang, E.S. Xue, X. L. Nan, T. Yue et al.: Scripta Mater, 68, 2013, 229-232.

[14] H. Watanabe, T. Mukai, M. Mabuchi, K. Higashi: Scripta Mater. 41, 1999, 209-215.

[15] T. Mohri, M. Mabuchi, N. Saito, M. Makamura: Mater. Sci. Eng. A 257, 1999, 287-294.

Acknowledgements

This paper was created within the project "**Creation of an international scientific team and incorporation to scientific networks in the area of nanotechnology and unconventional forming material. CZ.1.07/2.3.00/20.0038"**, which is financed by the European Social Fund and state budget of the Czech Republic.

european social fund in the czech republic
EUROPEAN UNION
MINISTRY OF EDUCATION, YOUTH AND SPORTS
OP Education for Competitiveness
INVESTMENTS IN EDUCATION DEVELOPMENT

R&D of centrifugal casting technology of intermetallic compounds for industrial applications.

Ing. David KAŇÁK, Ing. Karel MALANÍK, CSc.

VÚHŽ a.s., Dobrá 240, CZ 739 51 Dobrá, Czech Republic,

malanik@vuhz.cz, kanakd@vuhz.cz

Abstract

Inter-metallic alloys form an extensive class of materials, which is highly interesting from the perspective of their application in demanding environments, namely in the areas with high temperatures and high pressures under action of oxidation atmosphere. Big interest in these materials is caused by unique combination of their properties, such as high tensile strength at high temperatures, good resistance to oxidation and corrosion accompanied by their comparatively low density. Materials for use at high temperatures and pressures are primarily intended for components of energy and chemical equipments. Due to the application potential of these advanced materials, it was decided to start new project in VÚHŽ a.s. The aim of our project is verified centrifugal casting technology of intermetallic compounds based on Ni in operating conditions of foundry VÚHŽ a.s. This project is realized in cooperation with VŠB-Technical University of Ostrava and builds on previous results of research activities in this field at this institution. It is a comprehensive solution to increase the efficiency of research and development and accelerate the transfer of results into the application sphere, increasing the intensity and effectiveness of cooperation in research and development between industrial companies and research organizations. Implementation of this project will increase the quantity and quality of knowledge, applied research and experimental development of advanced technologies and materials that are applicable in the form of innovation in several sectors (metallurgy, energetics, etc.), thereby contributing to the production of goods and services with higher added value.

Keywords

Intermetallic, intermetallic compounds, centrifugal casting, melting, testing of material properties, technology processes optimizing.

1. COMPANY VÚHŽ a.s.

Nowadays the company VÚHŽ a.s. is modern and progressive producer of special products for many industry areas.

1.1 History, milestones

The joint stock company VÚHŽ Dobrá was established within the frame of so called voucher privatisation on the 1st May 1992 by transformation from the State-owned company “Iron and

Steel Research Institute", which was originally founded in Prague by General Directory of Czechoslovak metallurgical industry on the 1st April 1948 under the original name "Steel Research Institute". This institute moved in 1972 into newly premises built in Dobrá near Frýdek-Místek. In May 2007 VÚHŽ a.s. became a subsidiary company of the Třinec Steelworks a.s.

1.2 Parameters of the company

Turnover about 18 mil. EUR per year, number of employees about 300. Since 1992 is company VÚHŽ a.s. continually profitable, more than 60% turnover is exported among others to EU, China, Russia, India, USA or South Afrika.

1.3 Scope of activities

VÚHŽ a.s. operates at present in several spheres:

- designing and small batch production of measurement, control and automation technology, especially for metallurgical industry,
- small batch production of hot rolled sections, namely for automotive industry,
- designing and production of equipment for secondary metallurgy of steel and cast metals centrifugal casting of rolls and other castings for metallurgical plants, machine building industry, power engineering and food processing industry,
- production and machining of tools and moulds and their coating by CVD, PA CVD and PVD methods,
- research, development, testing, expert examination and consulting services for industry.

1.4 R&D activities / projects

In company VÚHŽ a.s. were realised numerous R&D projects, which were financed from the company own sources, as well as with use of public sources, such as subsidies, loans, etc. All of this projects were oriented on R&D of technology and new products and services for enterprising subjects. Many of results of this projects were applicated into industrial practise.

2. Ni_3Al based inter-metallic compounds

Nickel and nickel alloys have useful resistance to a wide variety of corrosive environments, typically encountered in various industrial processes such as in chemical processing petrochemical processing, aerospace engineering, power generation and energy conversion, thermal processing and heat treatment industry, oil and gas production, pollution control and waste processing, marine engineering, pulp and paper industry, agrichemicals, industrial and domestic heating, the electronics and telecommunication industries, and other.

2.1 Ni_3Al material

Nickel alloys containing an intermetallic phase Ni_3Al are very interesting thanks to their properties. The Ni_3Al-based alloy can be modified with chromium, molybdenum, zirconium, and boron additions for obtaining a combination of improved strength and ductility properties. The main characteristics of the material:

- highly ordered compound in the binary system Ni-Al with cubical structure of the type L12 maintains its orderliness till the temperatures close to melting temperature,
- high strength at elevated temperatures (main advantage) – strength properties increase with the increasing temperature approx. to 700°C,
- resistance to oxidation and corrosion,

- relatively low density.

3. R&D project within the programme ALFA

The output of the investigated project is a verified technology of centrifugal casting of Ni-Al based inter-metallic materials in industrial conditions of the VÚHŽ a.s. foundry shop. Investigation of the project is realised in collaboration with the VŠB - Technical University of Ostrava and it uses its previous results of research activity in this field.

3.1 Centrifugal casting

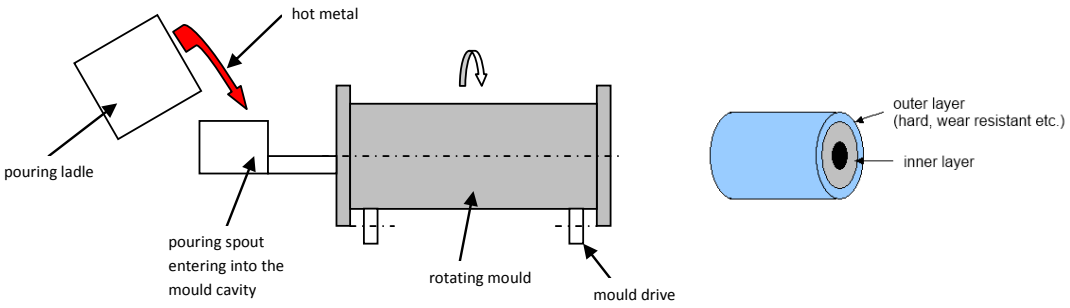

Fig. 1 Centrifugal casting - scheme

Centrifugal casting is a process of manufacture of castings, in which the molten metal (or other material) is poured into the rotating casting mould, in which the casting then solidifies and cools down. The mould and casting are separated from each other by thermal-insulation layer. The casting is after its solidification removed from the mould and it is further subsequently cooled down (in a controlled manner or freely on open air). Centrifugal casting makes it possible to produce parts of rotating shapes (circles, cylinders, rings), but also of shaped symmetrical castings, or double or multi-layered combinations of materials. Scheme of centrifugal casting is shown in **Fig. 1**.

3.2 Operating conditions of the VÚHŽ a.s. foundry shop

The VÚHŽ a.s. foundry shop has implemented technology of centrifugal casting with horizontal and vertical axis of rotation. The foundry it equipped with six horizontal casting machines and one vertical casting machine with the possibility of production of castings up to the diameter of 1100 mm and maximal mass of the casting 2000 kg. Metal is heated and prepared in electric medium frequency induction melting furnaces with nominal volume of crucible 500 kg (2 x), 1000 kg (1 x) 100 kg (1 x) a 40 kg (1x). For heat treatment of castings there are three car-type annealing furnaces with capacity of 2500 and 2x3000 kg.

3.3 Operating conditions of experiments in laboratory scale (VŠB)

There is a vacuum induction melting furnace with zirconium, graphite or steel crucible and maximal mass 800 g. For casting there is a technology of stationary casting and can be used also directional crystallisation.

3.4 Procedure of project solution

On the basis of the findings obtained by bibliographic searches a suitable composition of material for initial trials was proposed preparation and realisation of the series of model trials in laboratory conditions of the VŠB TU Ostrava, including development of methodology for these

trials. Realisation of laboratory experiments under various conditions at melting and casting of the samples (vacuum, argon, air, mould material, melting crucible, etc.) were done **(Fig. 2)** and all samples from laboratory trials were evaluated in an ongoing manner from the viewpoint of materials properties (chemical composition, gas contents, structural properties, etc.). Use of the findings from model trials for realisation of melting and castings tests performed in industrial conditions of the VÚHŽ a.s. foundry shop to realisation of industrial scale experiment **(Fig. 3)** with graded concentrations of alloying elements (influence of B, Cr, Zr, Mo, Nb…). The following parameters are monitored:

- chemical composition,
- structural characteristics,
- mechanical properties (including creep …).

On the basis of continuously obtained findings from laboratory analyses of model and industrial samples of castings we realised a continuous optimisation of:

- chemical composition of material and alloying,
- technological procedures for production, including protective atmosphere at melting,
- also the issues related to the mechanical machining and heat treatment of these material are solved.

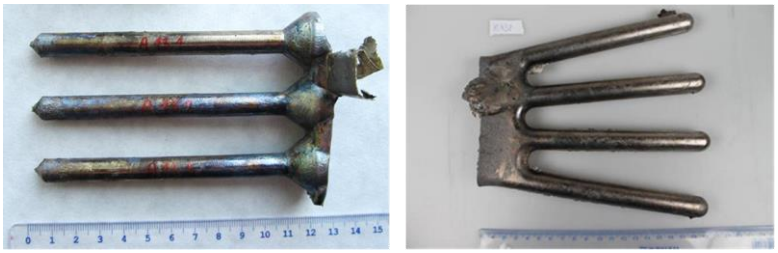

Fig. 2 Samples from laboratory castings (VŠB)

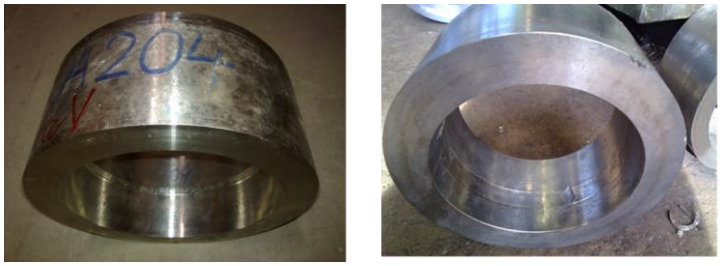

Fig. 3 Example of centrifugally cast sample in conditions of the VÚHŽ a.s. foundry shop

4. CONCLUSIONS

According to the R&D results achieved so far the application of the technology of centrifugal casting of Ni3Al based inter-metallic compounds in conditions VÚHŽ a.s. foundry shop appears to be perspective. In the final stage of the project we will perform an industrial verification of the final product made of this material in normal conditions of metallurgical plant (rolling mill).

Acknowledgements

This paper was created within the project "**Creation of an international scientific team and incorporation to scientific networks in the area of nanotechnology and unconventional forming material. CZ.1.07/2.3.00/20.0038"**, which is financed by the European Social Fund and state budget of the Czech Republic.

european social fund in the czech republic
EUROPEAN UNION
MINISTRY OF EDUCATION, YOUTH AND SPORTS
OP Education for Competitiveness
INVESTMENTS IN EDUCATION DEVELOPMENT

Microstructure and martensitic transformation in Ti-based alloys subjected to severe grain refinement

Wojciech MAZIARZ[a], Paweł CZAJA[a], Jan DUTKIEWICZ[a]

[a] *Institute of Metallurgy and Materials Scienc,e Polish Academy of Sciences, Reymonta Str. 25, 30-059 Kraków, Poland*

E - mail address w.maziarz@imim.pl

Abstract

Materials characterized by ultrafine and nanocrystalline microstructure show significantly different mechanical and structural properties as compared to those featuring coarser grain. This is well demonstrated in the case of Ni-Ti shape memory alloys (SMA), which fuse excellent mechanical properties with unique shape memory behavior and superelasticity. It has been shown that severe structure refinement of these alloys has an effect on the sequence of martensitic phase transformations and in consequence it may impact the thermo mechanical properties related to their shape memory behavior. Moreover it has been found that the self accommodation of martensitic plates is strongly dependent on the grain size. Ultrafine crystalline Ni-Ti SMA may be obtained by devitrification of an intermediate amorphous phase generated by high pressure torsion (HPT). HPT apart from equal channel angular pressing (ECAP) is one of the most commonly used methods of severe plastic deformation (SPD), which is employed to perform such an ultrafine and nano structuring. Other SPD modes such as cold rolling may also be implemented. In principle the SPD entails subjecting bulk materials to a large plastic deformation at relatively low homologous temperatures. The chief advantage of SPD is that it produces large samples, which are fully dense and may be manufactured from high purity precursors. This paper reviews recent progress in the area of Ti-based SPD structured materials. Some examples of β–Ti shape memory alloys deformed by cold rolling are also presented as a prospective route.

Keywords

Microstructure, Nanocrystals, Martensitic transformation, Shape Memory Alloys, SPD, TEM

1. INTRODUCTION

The first literature reports concerning bulk ultrafine-grained (UFG) materials appeared around the early 1990s and have immediately sparked a worldwide interest in this subject [1]. Over two decades later it still remains one of the primary focus of modern materials science and a new term Bulk Nanostructured Materials (BNMs) has been coined to highlight further grain size reduction. This interest is fueled by outstanding properties, unusual among larger grain analogues, and resulting from nanometer to several hundred nanometers sized grains. The average grain size is less than ~ 1 μm. Exceptional properties deriving from UFG microstructure such as high strength and ductility, superplasticity, elevated damping, record-breaking fatigue

life and endurance, attractive electric and magnetic properties have been demonstrated for numerous metals and alloys [2]. Needles to say that many of them pave the way for innovative structural and functional applications. Recent studies have identified over a 100 specific market areas where these materials could be put to practice. Emergence of additional applications, especially those related to extreme environments, is beyond a doubt. One of such examples are metal implants used for dental surgery and prosthetics with Ti and its alloys being the primary implant material. A very promising technique allowing for production of such nano- and submicrocrystalline materials is severe plastic deformation (SPD). It refers to various experimental modes but essentially it boils down to subjecting a work piece to a heavy straining under high pressure applied at relatively low temperatures. Enormous strains exerted on a material throughout this procedure yield outstanding grain refinement. The most striking feature of SPD is the fact that despite heavy straining imposed on a material there is no major change to its overall shape and volume. Another important advantage is that it may be utilized for production of bulk materials for real structural applications and at present SPD techniques are employed for manufacturing of various UFG products at commercial plant sites. This paper gives a short overview of microstructure and physical properties of UFG materials. Roll bonding as one of the SPD modes is briefly outlined. Some attention is given to the review of recent advancements in Ti - based UFG alloys. Finally selected aspects of β-Ti shape memory alloys subjected to cold rolling are presented and discussed.

1.1 Microstructure and properties of ultrafine grained polycrystalline materials

UFG materials are defined as polycrystals having the average grain size within the submicrometer (100 – 1,000 nm) and nanometer (<100 nm) ranges. Although SPD usually gives grains within the upper submicrometer limit, for pure metals it is about 100-200 nm, the materials it produces are often termed nanostructured materials. This is related to the fact that in some cases SPD can lead to grains in size below the lower range like 60 nm obtained in Ni_3Al by HPT, the same technique led to total amorphization of TiNi, and SPD consolidation of ball milled powders can even yield 15-20 nm grain size [3]. Another size factor is the presence of substructures in SPD processed solids, which are often smaller than 100 nm. They comprise subgrains, dislocation cells and X-ray coherent diffraction domains (crystallites), nanoparticles, nanotwins, grain boundary segregations etc. Apart from justifying the terminology these substructural features play a considerable role in the enhancement of mechanical properties, e.g. it has been established that grain boundary segregations and non-equilibrium boundaries can lead to stress values greatly exceeding those calculated from the Hall-Petch formula. These original phenomena are attributed to novel deformation mechanisms introduced by nano structuring. They encompass grain boundary sliding at low temperatures, generation of partial dislocations which may then involve dislocation glide, twinning, which has been detected at nanoscale even in solids possessing relatively high stacking fault energies. One of the most outstanding characteristics owing to this unique plasticity of NMs is the combination of ultra high strength and high ductility unparalleled (rarely coexisting) in conventional coarse grained metals and alloys. It opens up an entirely new field of structural and functional applications. For instance coincidence of both high strength and high ductility is crucial in order to achieve high impact toughness. For years engineers yearned for materials with improved impact toughness especially at low temperatures, since it is common knowledge that with the decrease of temperature the impact toughness of most metals and alloys degrades. This may pose a catastrophic risk when material is subjected to low temperature while under service conditions. Luckily this problem has now been overcome. Recent investigations have shown that both the strength and ductility of some NMs improve with decreasing testing temperatures and increasing strains. It has also been demonstrated that impact toughness of SPD nanostructured

Ti gets better at low temperatures of -70 ºC and -196 ºC [4]. The combination of high strength and ductility-elongation renders also outstanding properties (adds another functional dimension) to shape memory alloys capable of superelasticity and shape memory effect. But the microstructure refinement responsible for improving the mechanical properties may at the same time affect the characteristic phase transformation temperatures since it is known that they strongly depend on the grain size. For instance it has been observed that the grain size strongly influences the transformation sequence in nanocrystalline NiTi, which is the following: B2→R phase→B19'. Moreover self accommodation of martensitic plates can occur differently depending on the nano grain sizes [5]. In coarse grained materials the twinning periodicity is usually in the range of several 10 - 100 nm. This leads to self accommodated martensitic arrangements composed of groups of different twinned variants. On the other hand in nanostructured solids the twinning periodicity is significantly larger than the crystallite size. This then may have an effect on phase stability and morphology of martensite [6]. Some influence of microstructure refinement on the kinetic behavior and corrosion resistance of SPD processed metallic materials has also been reported [7]. At this point it should be emphasized that SPD can produce uncontaminated nanomaterials with no porosity and with no nanovoids. This is of crucial importance in terms of strength and ductility enhancement and it is often desirable from scientific and engineering points of view.

1.2 SPD processed Ti-base alloys

The unexpected combination of high strength and ductility was observed for the first time in SPD processed Cu and Ti [8]. Titanium and its alloys are nowadays widely used as implants for biomedical applications such as traumatology, orthopedics and dentistry. This stems from excellent biocompatibility, good corrosion resistance and specific strength of Ti compared to other metals. The challenge here is however to increase the specific strength of the implant, thereby enabling it to withstand complex loads, and at the same time reduce the size permitting less invasive surgery. Another consideration is to use titanium in pure form with no alloying elements, provided that its strength can be increased twofold or more. Both of these may be achieved through SPD as exemplified by recent studies. It has been demonstrated that SPD leads to an increase of hardness while maintaining good ductility in CP Ti [9]. Experimental results supply evidence that the Hall-Petch relation is followed up to the barrier of 10 nm grain size, above which materials tend to soften. The strength can be further increased as in the case of HPT processed Ti, which was then subjected to low temperature annealing (250 ^{o}C and 300 ^{o}C). The ultimate strength of such Ti exceeded 1200 MPa, which is close to many Ti alloys, and the ductility was still sufficient [10]. This phenomenon is attributed to the decrease of lattice distortions induced by short term annealing, which does not involve observable grain growth. Nanostructuring may also significantly increase the fatigue strength of CP-Ti as compared to the coarse grained Ti-6AL-4V alloy permitting its use for enhanced biomedical applications [11]. Corrosion resistance of Ti appears to benefit from nanostructuring too [12]. The study of friction coefficient of CP Ti showed that the UFG microstructure decreases its tendency to seizure and galling and should lead to lower friction coefficient and higher wear resistance than those in coarse grained Ti [13]. The choice of the technique and the state of microstructure (CG or UFG) prior to processing may have an impact on the properties of the final product. The ECAP processed Ti rod with UFG microstructure subjected to further CR has shown higher strength and ductility than the work piece subjected only to a single step processing [14]. Near ambient temperature large-strain machining has however shown that the two stage process may be bypassed. Chip forming from CP Ti using this technique has produced sufficient UFG microstructure without additional processing [15].

2. EXAMPLE OF OWN RESEARCH

2.1 Ni-free shape memory alloys

SPD is equally important with respect to structuring of Ti alloys. It may support the development of new Ni and other toxic elements free β Ti alloys for biomedical purposes. In this respect more attention should be given to SPD processed β phase since it has been reported to split between two sub-phases under high intensity deformation involving ARB [16]. The β-type Ti-base alloys have attracted attention as new biomedical shape memory and superelastic alloys. Also the β-type Ti-base alloys exhibit excellent cold workability; a thickness reduction of > 90% is easily achieved by cold working at room temperature, so they can be easily fabricated into wires or sheets with dimensions suitable for actual applications. The origin of their shape memory behavior is the reversible martensitic transformation between the β parent phase and the α'' martensite phase. In order for these alloys to exhibit the shape memory effect, it is necessary to obtain the β phase, which is achieved by the addition of β phase stabilizers such as Mo, Nb and Ta to Ti. However, the β-type alloys are sensitive to aging at intermediate temperatures (373–673 K), where the thermal ω phase is formed. The nucleation and growth of ω phase when exposed to temperatures above 373 K can suppress martensitic transformation and cause embitterment.

2.2 Microstructure and martensitic transformation in $TiTa_{30+x}$ (x=0,4,8) alloys

The work concerned an optimization of composition and fabrication technology of β-Ti shape memory alloys. The fabrication and characterization of Ti-Ta alloys with the various Ta content from 30 up to 38 at.% was performed. The alloys were plastically deformed at the room temperature with to 95% size reduction. It was determined that the deformation rate influences on deformation and two stage of strengthening was observed. The plastic deformation causes almost ten times the grain size reduction in compare to the annealed samples and suppress the nucleation of ω phase (Fig. 1).

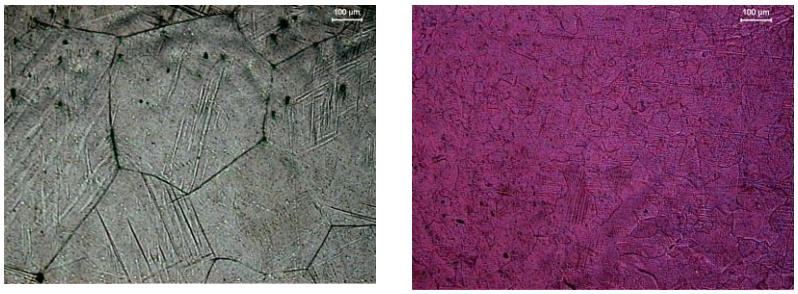

Fig. 1 Comparison of grain size in alloys without a) and with b) plastic deformation process

The microstructure observation revealed a differ morphology of martensite (plates, needles) but the same orthorhombic structure with the lattice parameter as a=3.830, b=4.957, c=6.86 (Fig. 2). The DSC measurements of solution treated alloys showed that M_s temperature are in the range from 368 to 383°C and with the weak correlation between M_s and the content of Ta.

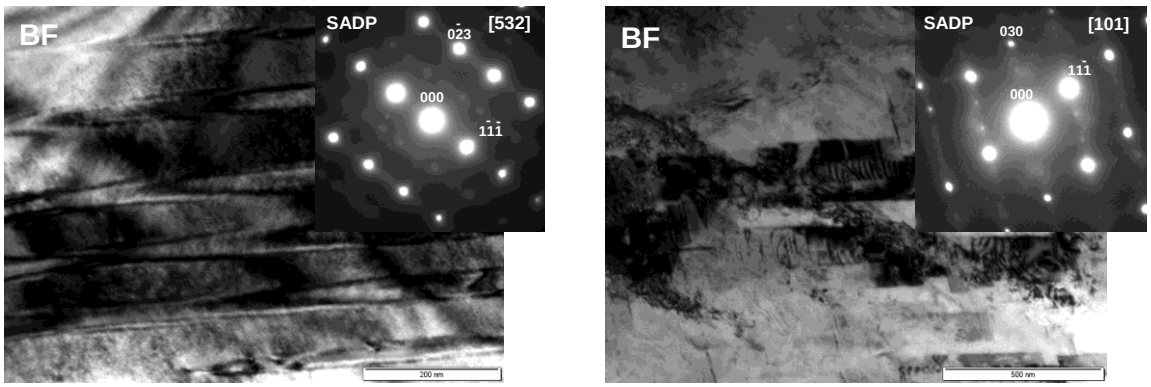

Fig. 2 Differ morphology of martensite (needles, plates) but the same orthorhombic structure with the lattice parameter as a=3.830, b=4.957, c=6.86 in aloys after plastic deformation a solution treatment

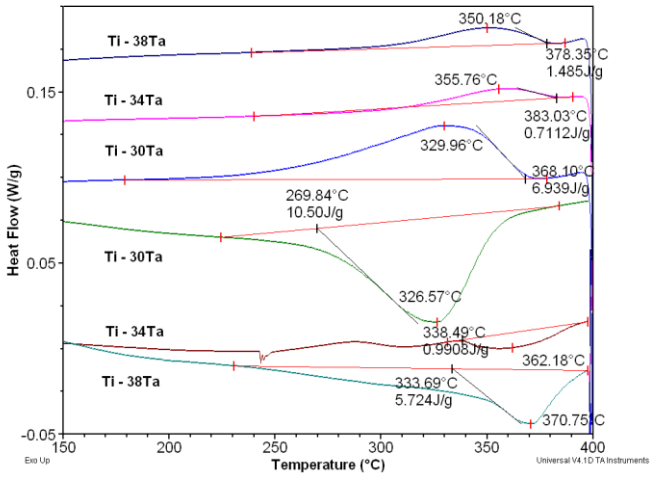

Fig. 3 Set of DSC curves recording during cooling and heating cycles for alloys after plastic deformation and solution treatment

3. SUMMARY

Using HPT, CR or ECAP nanostructured Ti-base shape memory alloys can be obtained via the devitrification of an intermediate amorphous structure. In nanocrystalline NiTi, a unique morphology of the martensite occurs that is caused by the minimization of the strain and interface energy opposing the martensitic transformation. When NiTi is subjected to severe plastic deformation, ultrahigh strength and good ductility is achieved in combination with enhanced functional properties of the shape memory effect and superelasticity. With respect to fracture and fatigue, nanocrystalline materials processed by severe plastic deformation open up a field that is rich in opportunities for future research. The β-Ti alloys posses a superior cold workability and can be used for sever plastic deformation process. This is very perspective for further investigations in this field of interest.

4. LITERATURE

[1] T. G. Langdon. Research on bulk nanostructured materials in Ufa: Twenty years of scientific achievements. Materials Science and Engineering A 503 (2009) p. 6–9.

[2] R. Z. Valiev et al. Producing Bulk Ultrafine-grained Materials by Severe Plastic Deformation. JOM 2006 58(4) p.33-39

[3] H. Shen, Z. Li, B. Guenther, A.V. Korznikov, R. Z. Valiev, Influence of powder consolidation methods on the Structural and Thermal Properties of a Nanophase Cu-50wt%Ag Alloy, Nanostr. Mater., 6 (1995) 385-388.

[4] V. V. Stolyarov, R. Z. Valiev Enhanced low-temperature toughness of nanostructured Ti. Appl. Phys. Lett. 88 (2006) 041905

[5] T. Waitz, W. Pranger, T. Antretter, F. D. Fischer, H. P. Karnthaler. Mater. Sci. Eng. A Vol. 481-482 (2008) p.479.

[6] T. Waitz. Bulk Nanostructured Shape Memory Alloys. Ciencia e Tecnologia dos Materiais, Vol. 20, 1/2, 2008.

[7] Y. T. Zhu, T. C. Lowe, T. G. Langdon. Performance and applications of nanostructured materials produced by severe plastic deformation. Scripta Materialia 51 (2004) 825-830.

[8] R. Z. Valiev et al. J. Mater. Res. 17 (2002) p. 5.

[9] M. Greger, L. Kander, V. Masek, P. Kociscakova. Structure and properties of ultra-fine grain titanium used for special applications. COMAT 2010 Recent trends in structural materials. 25-26 November 2010, Pilsen, Czech Republic.

[10] A. V. Sergueeva, V. V. Stolyarov, R. Z. Valiev, A. K. Mukherjee. Advanced mechanical properties of pure titanium with ultrafine grained structure. Scripta Materialia 45 (2001) 747-752.

[11] Stolyarov VV, Zhu YT, Aleksandrov IV, Lowe TC, Valiev RZ. Mater. Sci. Eng. A 2003;343:43

[12] A. Balyanov, N. A. Amirkhanova, V. V. Stolyarov, T. C. Lowe, R. Z. Valiev, Y. T. Zhu. Scripta Mater. 2004; 51 p. 225-9.

[13] V. V. Stolyarov, L. Sh. Shuster, M. Sh. Migranov, R. Z. Valiev, Y. T. Zhu. Reduction of friction coefficient of ultrafine-grained CP titanium. Mater. Sci. Eng. A 371 (2004) 313-317.

[14] V. V. Stolyarov, Y. T. Zhu, G. I. Raab, A. I. Zharikov, R. Z. Valiev. Effect of initial microstructure on the microstructural evolution and mechanical properties of Ti during cold rolling. Mater. Sci. Eng. A 385 (2004) 309-313.

[15] M. Ravi Shankar, Balkrishna C. Rao, Seongeyl Lee, Srinivasan Chandrasekar, Alexander H. King, W. Dale Compton. Severe plastic deformation (SPD) of titanium at near-ambient temperature. Acta Materialia 54 (2006) 3691–3700.

[16] A. D. Vulcan, D. Raducanu, V. D. Cojocaru, I. Cinca, L. Angelescu. X-ray diffraction of a Ti-Ta-Nb alloy processed by severe plastic deformation. U. P. B. Sci. Bull. Series B. Vol. 74. Iss. 2. 2012.

Acknowledgements

This paper was created within the project "**Creation of an international scientific team and incorporation to scientific networks in the area of nanotechnology and unconventional forming material. CZ.1.07/2.3.00/20.0038"**, which is financed by the European Social Fund and state budget of the Czech Republic.

INVESTICE DO ROZVOJE VZDĚLÁVÁNÍ

Experimentalní možnosti výzkumu SPD u vytvrzovatelných slitin hliníku

Experimental possibilities of SPD investigation in age-hardening aluminium alloys

Vladivoj OČENÁŠEK

SVÚM a.s., Podnikatelská 565, 190 11 Prague 9 – Běchovice, Czech Republic, ocenasek@svum.cz

Abstract

In comparison with non-age-hardening aluminium alloys, the investigation of the SPD effect on structure and properties of age-hardening aluminium alloys requires a quite specific approach to carrying out experiments. When the experiments aim at reaching optimum properties (it does not mean always the maximum ones), the relations between as received - and final structure, heat treatment (solution annealing, natural ageing, artificial ageing) and deformation applied leading to an ultra-fine-grained structure shall be taken in consideration. The paper deals with the possibilities which respect these demands and lead to the better utilizing of properties of aluminium age-hardening alloys. The effect of various technological parameters on the course of experiments is analysed. Examples of SPD experiments, that are substantially meaningless and of experiments showing that an optimum hardening effect can be reached owing to the interaction of a plastic deformation and precipitation hardening, are given.

Keywords

Severe plastic deformation, age-hardening aluminium alloys, heat treatment, microstructure

1. ÚVOD

Slitiny hliníku jsou velmi často předmětem studia intenzivní plastické deformace k získání jemnozrnné struktury s velikostí zrna pod 1 μ, případně pod 500 nm. V odborných článcích, které se zabývají SPD u hliníkových slitin, se můžeme setkat s celou řadou slitin, řadou výchozích stavů materiálů, deformačních metod a postupů [1-7]. Vliv SPD lze sledovat z různých důvodů. Cílem může být například jak pouhé studium vlivu intenzivní plastické deformace na zjemňování struktury modelového materiálu, tak výzkum zaměřený na použití materiálu pro určité aplikace. Deformovaný materiál je často podrobován dalším testům, například z pohledu tepelné stability (creep, superplasticita) nebo dalších podmínek použití (korozní odolnost, únavové namáhání). Experimentální materiál pro tyto zkoušky mívá různý původ a historii, velmi často prochází před vlastním experimentem k tepelně mechanickému zpracování, které připraví definovaný výchozí stav. V řadě případů se však stává, že výchozí materiál má nedefinovaný původ a stav struktury nebo jsou sledovány stavy struktury, které nemají praktický význam. To může mít zásadní vliv jak na interpretaci výsledků deformačních zkoušek, tak také na jejich aplikovatelnost při případném využití v praxi. V tomto příspěvku je

věnována pozornost experimentálním možnostem studia SPD v případě vytvrzovatelných slitin hliníku. V příspěvku je upozorněno na případy, kdy provádění náročných deformačních zkoušek nemá vzhledem k výchozímu stavu struktury a metodice deformačních zkoušek a vzhledem k dosaženým vlastnostem dané vytvrzovatelné slitiny praktický význam.

Výsledky deformačních zkoušek nezávisí pouze na průběhu a parametrech zkoušení ale výrazným způsobem jsou ovlivněny i historií přípravy materiálu před vlastními zkouškami. Historie přípravy experimentálního materiálu (jeho struktury) významně ovlivňuje jak deformační podmínky experimentů, tak i vlastnosti, kterých je dosaženo po SPD. Neznalost původu experimentálního materiálu (tj. historie jeho výroby), nebo nevhodné či smysl nemající stavy struktury materiálu určeného k deformačním zkouškám, mohou proto znehodnotit výsledky, znemožnit jejich reprodukovatelnost, nebo minimálně ztížit jejich interpretaci. Na Obr. 1 je uvedeno schéma běžného technologického postupu výroby hliníku a jeho slitin. Ten se obvykle sestává z lití, vysokoteplotního žíhání (homogenizace), tváření za tepla, tváření za studena, mezioperačního žíhání a konečného tepelného zpracování. V závislosti na typu slitiny a typu výrobku lze některou z uvedených operací samozřejmě vypustit. K SPD experimentům lze použít materiál po každé z uvedených operací. V tomto příspěvku se budeme zabývat slitinami, jejichž velmi dobré mechanické vlastnosti jsou určeny tepelným zpracováním, které se sestává z rozpouštěcího žíhání a precipitačního vytvrzování.

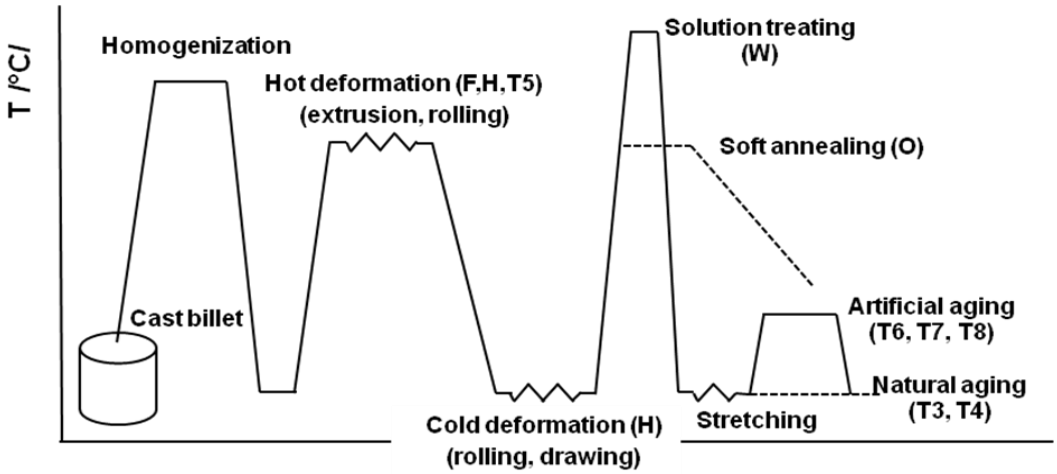

Fig. 1 Scheme of common technological procedure by preparing aluminium products

2. VYTVRZOVATELNÉ SLITINY HLINÍKU POUŽÍVANÉ PŘI STUDIU SPD

Mezi vytvrzovatelné slitiny často sledované metodami SPD patří slitiny řady 6XXX (legované Mg a Si), 7XXX (legované Zn, Mg a Cu), případně 2XXX (legované Cu, Mg, Ni). Jmenujeme-li alespoň některé z nich, tak to jsou slitiny 6061, 6082, 7075, 2024 a 2618. V závislosti na obsahu legujících prvků a technologických parametrech přípravy se potom mění složení intermetalických fází, vytvrzujících fází, deformační odpor a tím konečné vlastnosti po SPD. Vzhledem k velkému rozsahu SPD experimentů provedených doma i v zahraničí se dále budeme věnovat pouze některým aspektům těchto zkoušek.

3. STAV STRUKTURY PRO DEFORMAČNÍ ZKOUŠKY METODAMI SPD

Pro průběh deformačních zkoušek je výchozí stav struktury zásadní, protože se od něj odvíjí strategie experimentu. Nebo naopak, pro určitou strategii experimentu je nutné zvolit vhodnou výchozí strukturu. Podstatné je nejen to, zda je materiál v měkkém nebo zpevněném stavu ale i to, v jaké formě jsou přítomny intermetalické fáze nebo precipitáty. Rovněž je nutné odhadnout, k jakým změnám struktury může dojít v průběhu zkoušek, které jsou rozloženy do relativně dlouhého časového úseku. V případě vytvrzovatelných slitin hraje důležitou roli nejen výchozí stav struktury, ale i požadavky kladené na konečnou strukturu (teplotní stabilita, superplastické chování, vysoká pevnost za normální teploty při dostatečné plasticitě). Na Obr. 2 jsou znázorněny některé kombinace výchozích stavů struktury a parametrů deformačních podmínek.

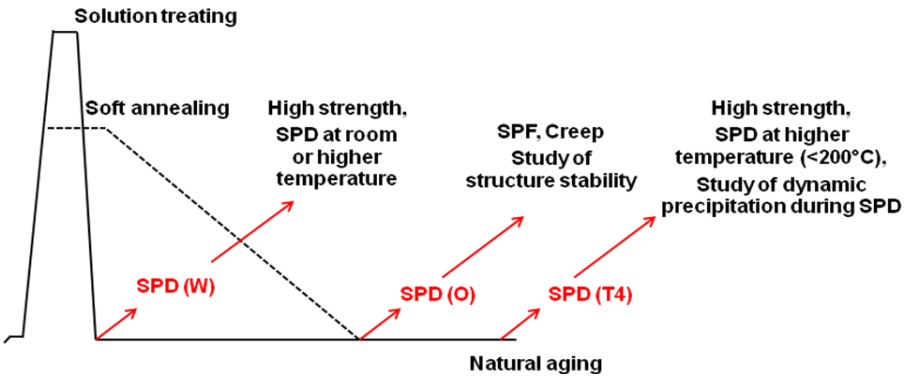

Fig. 2 Possibilities of initial state of structure by SPD experiments

V případě vytvrzovatelných slitin je situace složitější než u slitin nevytvrzovatelných. Pokud chceme využít potenciálu těchto slitin, je nutné provést rozpouštěcí žíhání, které se pohybuje v rozmezí teplot 475 °C (slitina 7075) až po 530°C (slitiny řady 6XXX). Pokud by byla SPD provedena před rozpouštěcím žíháním, pak uložená deformační energie povede při rozpouštěcím žíhání k rekrystalizaci a ztráty struktury, která je cílem SPD. Dosáhnout tímto způsobem velikosti zrna pod 1 μm, případně pod 500 nm je prakticky vyloučené. Pokud je cílem kromě dosažení struktury zrna o rozměru několik stovek nanometrů dosáhnout i vysokých pevnostních hodnot odpovídajících zkoumané slitině, je nutné deformaci provádět až po rozpouštěcím žíhání (stav W nebo T4).

V případě, že k deformaci nedojde okamžitě po ochlazení z teploty stárnutí, je nutné počítat s tím, že slitiny budou přirozeně stárnout, a tím zpevňovat. Přírůstek zpevnění přirozeným stárnutím může tvořit 50 až 100% procent zpevnění dosaženého umělým stárnutím. V období, kdy bude materiál postupně jednotlivými průchody deformován, bude tak zpevňovat, a to jak deformačně, tak precipitačně. Deformace přitom vlastní precipitační zpevnění urychluje. Z toho vyplývá pro vytvrzovatelné slitiny jedno zásadní omezení, a to, že deformaci vícenásobným průchodem lze provádět za studena pouze v omezeném rozsahu (1-2 průchody). Proto je výhodnější provádět deformační zkoušky za zvýšené teploty. Teplota deformace by přitom neměla překročit teplotu umělého stárnutí, aby byl využit precipitační potenciál sledované slitiny. V tomto případě se budou teploty deformace pohybovat většinou pod teplotou 200°C. Dosažení maximálních pevnostních hodnot pak závisí na celkové době, po kterou byla slitina na teplotě deformace (tj. včetně doby ohřevu na deformační teplotu). Vzhledem k tomu, že doby umělého stárnutí se pohybují v závislosti na typu slitiny a teplotě stárnutí v intervalu od 4 do 12 hodin, tak deformace řadou průchodů (například metodou ECAP) se obvykle do tohoto časového intervalu vejde. Příklady zpevňování metodou ECAP různými postupy jsou uvedeny na Obr. 3 a 4.

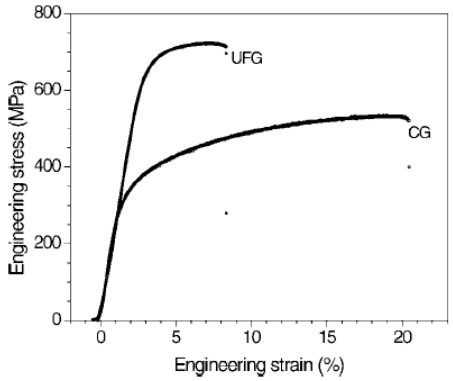

Fig. 3 Alloy 7075 Solution treated (W), ECAP, 2 passes at room temperature, 1 month NA [2]

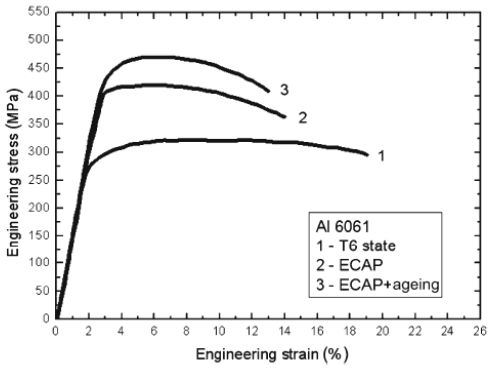

Fig. 4 Alloy 6061, Solution treated 530°C/1h./ WQ, ECAPed by 4 passes at 110°C+ ageing at 130°C/24 h.,initial grain size 100 μm [3]

Z uvedeného rovněž vyplývá, že nemá smysl sledovat účinky SPD na vytvrzovatelných slitinách bez provedení tepelného zpracování. Deformační zpevnění dosažené pouze SPD je menší než zpevnění precipitační a takto připravený materiál by měl naději na praktické využití pouze v případě, že jemné zrno by bylo z nějakého důvodu rozhodujícím parametrem. Výsledné deformované struktury po SPD, které byly u vytvrzovatelné slitiny připraveny z měkkého stavu přestárnutím mají sice malé zrno, ale mechanické vlastnosti jsou nižší, než mají tyto slitiny po precipitačním vytvrzení. Kromě toho mohou mít i horší plastické vlastnosti. Proto je nutné deformační zkoušky u vytvrzovatelných slitin hliníku provádět tak, aby se využilo jak deformačního zpevnění intenzivní plastickou deformací, tak zpevnění precipitačního.

Určitou výjimkou je případ sledování SPD u slitin, které lze využít pro superplastické tváření. Typickým případem je slitina 7075. V tomto případě je výchozím stavem materiálu pro zkoušky SPD stav měkký dosažený pomalým ochlazováním z teplot kolem 450°C rychlostí menší než 50°C/hod. Vlastní tepelné zpracování spojené s vytvrzením pro dosažení optimálních mechanických vlastností pak následuje až po superplastickém tváření. Cílem SPD je v tomto případě získat jemnozrnnou strukturu, která zlepší parametry superplastického tváření ve srovnání s běžným způsobem přípravy jemnozrnné struktury, kdy se dosahuje velikosti zrna na úrovni 5 až 15 μm). Příklad zjemnění zrna pro superplastické tváření pomocí SPD u slitiny 7075 je uvedeno na Obr. 5.

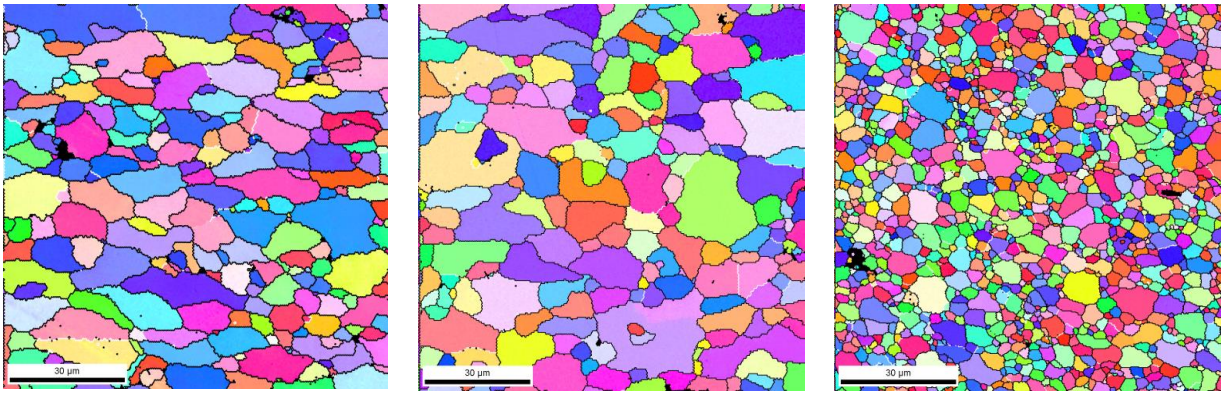

a) b) c)

Fig. 5 Structure of 7075 alloy prepared for superplasticity test by ECAP, a) befor ECAP, d=15-25 μm, b) after 1. Pass + T6, d= 8 μm, c) after 6 passes, d=3 μm [5]

4. ZÁVĚR

Cílem příspěvku bylo upozornit na některé zvláštnosti přípravy experimentálního materiálu a experimentální podmínky pro sledování SPD na vytvrzovatelných slitinách hliníku. Vzhledem k požadavkům na vlastnosti jemnozrnných struktur je nutné definovat výchozí stav struktury a volit deformační podmínky tak, aby zohlednily specifické charakteristiky vytvrzovatelných slitin. Deformační zkoušky je nutné provádět tak, aby bylo využito jak intenzivní plastické deformace, tak precipitačního vytvrzení.

5. LITERATURE

[1] L. Lodgaard.: Precipitation of dispersoids containing Mn and/or Cr in Al-Mg-Si-alloys, Thesis, (2000), NTNU Trondheim

[2] Y. Zhao at al.: Microstructures and mechanical properties of ultrafine grained 7075 Al alloy processed by ECAP and their evolutions during annealing, Acta Materialia 52 (2004) 4589-4599

[3] X. Sauvage, M. Yu. Murashkin, R. Z. Valiev.: Atomic scale investigation of dynamic precipitation and grain boundary segregation in a 6061 aluminium alloy nanostructured by ECAP, Kovove Mater. 49 (2011) 11-15

[4] J. A. Wert, N. E. Paton, C. H. Hamilton, and M. W. Mahoney.: Metall. Trans.,12A (1981) 1267

[5] V. Ocenasek at al.: Effect of heat treatment on the structure of the aluminium alloy AA7075 subjected to intensive plastic deformation by ecap, Conf. Metal 2008, CD ROM

[6] K. Turba, P. Malek, E. F. Rauch, and M. Cieslar: The optimization of ECAP conditions to achieve high strain-rate superplasticity in a Zr- and Sc-modified AA 7075 aluminum alloy, Int. J. Mater. Res. (Zeitschrift für Metallkunde) 100, 2009, 851 – 857.

[7] P. V.Liddicoat at al.: DOI:10.1038/ncomms1062 (2010)

Poděkování

Tento příspěvek byl vytvořen v rámci projektu Tvorba mezinárodního vědeckého týmu a zapojování do vědeckých sítí v oblasti nanotechnologií a nekonvenčního tváření materiálu CZ.1.07/2.3.00/20.0038, který je spolufinancován z Evropského sociálního fondu a státního rozpočtu České republiky.

european social fund in the czech republic
EUROPEAN UNION
MINISTRY OF EDUCATION, YOUTH AND SPORTS
OP Education for Competitiveness
INVESTMENTS IN EDUCATION DEVELOPMENT

New types of magnesium alloys for ECAP processing

Stanislav RUSZ [a], Lubomír ČÍŹEK [a], Jan KEDROŇ [a], Stanislav TYLŠAR [a], Michal SALAJKA [a]

[a] *VSB – Technical university of Ostrava, 17. listopadu 15, CZ 708 33 Ostrava – Poruba, Czech Republic, stanislav.rusz@vsb.cz*

Abstract

The technology ECAP – Equal Channel Angular Pressing, belongs to technologies of accelerated development and represents top items of severe plastic deformation methods to reach ultra-fine granularity structure. This concerns specifically forming of non-ferrous metals and their alloys. This technology was therefore applied namely for aluminium alloys. In this article a new type of magnesium alloys for ECAP processing are presented. Samples with dimensions 15x15x55 mm for ECAP processing were used. This paper describes namely on ECAP technology investigations that have been oriented on overall objectives of acquiring new knowledge concerning strengthening, influence of stress conditions, mechanical properties and microstructure of magnesium alloys given above. Measurement of Vickers hardness for determination of mechanical properties and methods of light microscopy for the study of microstructures were used.

Keywords

Severe plastic deformation, ECAP process, magnesium alloys, mechanical properties, structure

1. INTRODUCTION

The interest in application of magnesium alloys in wide spectrum of industries rises from traditional used alloys as the main alloying component which is continuously improving and still new types are being developed [1,2,3,4]. Non-ferrous metals and their alloys can be recycled very well and they replace more and more the steels.The increasing use of magnesium alloys is caused by the progress in the manufacturing of new reliable alloys with the addition of Zr, Ce, Cd, RE and very light alloys are made from Li [1,2,5].

The properties of magnesium alloys are connected with microstructure that is influenced by metallurgical and technological aspects. Recently, however, increases also utilisation of the formed magnesium alloys, namely application of SPD methods. AZ91 alloy is widely used as cast magnesium alloy. Contemporary AZ61, AZ31 alloys and many new advanced alloys (for example WE43 and Mg-Zr alloys) are used for utilisation of cast and formed magnesium alloys. The experimental part deals with determination of properties and structure of AZ31, WE43 and Mg-Zr magnesium alloys after ECAP processing.

2. EXPERIMENTAL MATERIALS AND PROCEDURES

Magnesium alloys AZ31, WE45 and Mg-Zr supplied in the form of bars with dimensions Ø20 – 600 mm length (rod with diameter 50 mm was extruded to 20 mm). Chemical composition of used alloys is given in Table 1. The ECAP technology is presented in the works [6-9]. The principle and working site of ECAP method shows Fig. 1.

Table 1 Chemical composition of used alloys (in wt %)

Used materials	Al	Cu	Mn	Zn	La	Y	Nd	Zr
AZ31	2,96	0,002	0,1	0,2	-	-	-	0.003
WE43	0,007	0,03	0,002	0,008	0,009	4,01	2,04	0,494
Mg-Zr	-	-	0,016	0,004	0,003	-	-	0,453

Fig. 1a shows the principle of ECAP method. Example of results modeling of the development of magnitudes of strain intensity at ECAP method for aluminium AlMn1Cu alloy [7] is shown in Fig. 1b. Experimental working site with hydraulic press of the type DP 1600 KN shows Fig. 1c and detail of the forming tool with reheating sleeve shows Fig. 1d.

After rod extruding and cutting the specimens with dimensions 15 × 15 – 60 mm were used at experiments for the ECAP process. The ECAP processing at the temperature 220°C for AZ31 alloy and 240°C for WE43 and Mg-Zr alloys was realised. At this temperature the total number of 3 passes was applied in dependence on the evolution of extrusion (for AZ31 and Mg-Zr alloys the 1st - 3rd pass and for WE43 the 1st pass - after the next pass of that alloy the sample was destroyed). Samples were then divided into individual series for manufacture of specimens for mechanical testing and metallographic evaluation.

The hardness test for determination of mechanical properties was performed on the equipment HPO250.

The samples for metallographic evaluation were prepared in usual manner. Polishing of samples was made in two stages. In the first stage the samples were polished on cloth with use of the Al_2O_3 based polishing suspension. In the second stage the polishing was made on very fine velvet cloth with short fibres. Diamond powder with grain size of 1 μm was used as polishing material. Diamond was applied by spraying and cloth was regularly wetted by alcohol-based liquid.

The samples were then etched by Nital. Duration of etching varied from 5 to 10 seconds. Light microscope NEOPHOT 2 was used for evaluation of microstructure of alloys.

3. RESULTS AND DISCUSSION

3.1 Hardness test

Mechanical properties were tested by method of Vickers. Results of Vickers hardness HV5 are shown in Tab. 2. Average hardness of the initial state of the alloy AZ31 was 56 HV5. In the initial material for the ECAP process produced by casting with subsequent extrusion a considerable heterogeneity was determined, which was manifested by the obtained values of hardness. After the 3rd pass through the ECAP tool the average value of hardness of 69 HV5 was achieved. Hardness increased approx. by 30%. In the case of AZ31 alloy these values increased from the 1st to 3rd pass. This increase is more significant between the initial state and the 1st pass, while between the 2nd and 3rd passes the increase was only slight.

In the case of WE43 alloy the increase of hardness was more significant than in the case of *AZ31 and WE43 alloy.*

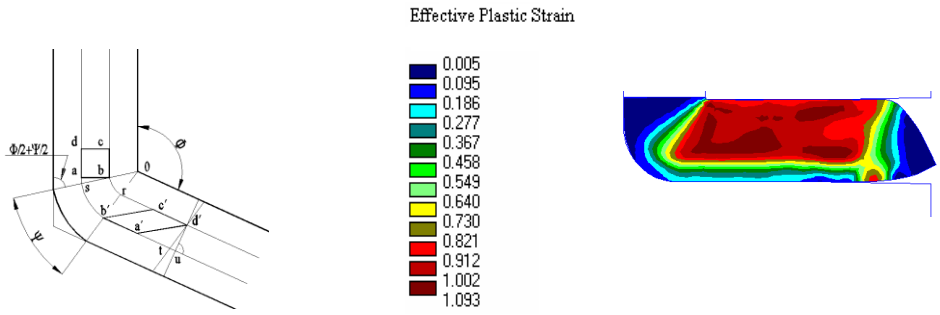

a) b)

c) d)

Fig. 1 Principle and working site of ECAP method a) Principle of ECAP, where Φ is the angle of transition of two channels and Ψ curvature of transition, b) Developments of strain intensity for channel radii R_1 = 5.5 mm, R2 = 0.2 mm, c) Experimental working site with hydraulic press of the type DP 1600 KN – Basic equipment and control system, d) detail of the forming tool with reheating sleeve [7].

In the case of Mg-Zr alloy these values increase from the 1st to 3rd passes. This increasing is more significant between initial state and the 1st pass while between the 2nd and 3rd passes increased slightly.

Table 2 Hardness of used alloys.

Alloy/No of passes	Initial state	1st pass	2nd pass	3rd pass
AZ31	56	64	67	69
WE43	70	102	-	-
Mg-Zr	27	36	35	35

3.2 Metallographic analysis

Selected typical structures of the used alloys AZ31, WE43 and Mg-Zr alloys as cast state are presented in Fig. 2. Microstructure of the AZ31 alloy is created by primary solid solution α with a little portion of the phases ($Mg_{17}Al_{12}$) at grain boundaries (Fig. 2a). Microstructure of the alloy WE43 in initial state is shown in Fig. 2b. In the region of grain boundary the occurrence of intermetallic phases may be expected. In the next examination we will apply a micro-analysis performed by SEM to specify that.

Microstructure of the alloy Mg-Zr in initial state is shown in Fig. 2c. This microstructure is formed by large polyedric grains of Mg based solid solution with dimensions in the range of 100 – 500 μm, which contain oblong relief. Due to the fact that the alloy with this composition has been developed recently and its structure is not described in available literature it can be assumed that these can be grains of magnesium based solid solution, in which a precipitation of fine minority phases could have occurred during solidification due to influence of positive solubility coefficient [10].

a) b) c)

Fig. 2 Microstructure of used magnesium alloys as cast state: a) AZ91, b WE43, c) Mg-Zr.

Microstructure of AZ31 after hot extrusion and ECAP processing is shown in Fig. 3. It is possible to assume from the analysis of initial states of the alloy AZ31 (see Fig. 2c) that structures are formed by irregular grains of solid solutions of tramp elements dissolved in magnesium matrix. In comparison with the initial state we may observe substantial grain refinement (see Figs. 3b – c), including their more uniform size. The grain size in initial state (see Fig. 2c) is classified (according to ASTM) as G8 and extrusion (the 1st - 3rd pass, see Figs. 3b – c) as G12.

Microstructure of the alloy WE43 after applied deformation (the 1st pass) is shown in Fig. 4a. Microstructure of the alloy WE43 in initial state is formed mostly by equi-axed grains with smaller size of grains than in the case AZ31 alloy.

Microstructure of the alloy Mg-Zr after applied deformation (the 1st - 3rd pass) is shown in Fig. 1b-d. As it is seen from this figure fine grain microstructure vas occurred after deformation. The most change of microstructure after the 1st pass is detected while after the 2nd and the 3rd pass refinement shows lower value.

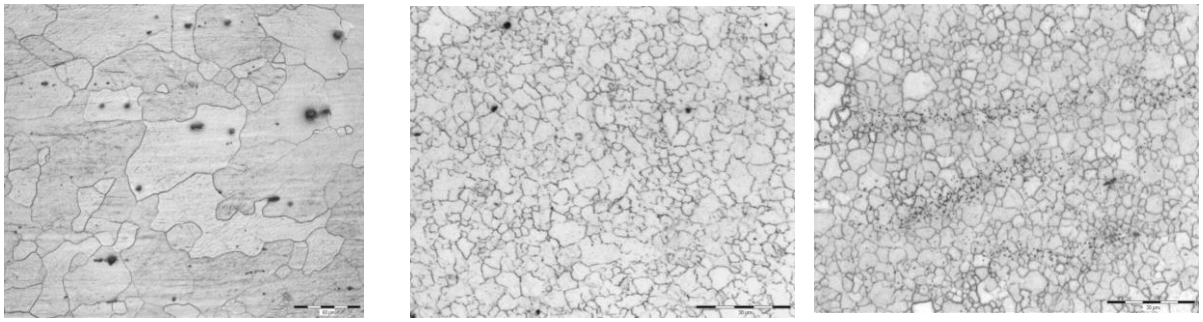

a) b) c)

Fig. 3 Structure of the alloy AZ31 a) initial state after extrusion, b) after the 2nd pass, c) after the 3rd pass.

a) b) c)

Fig.4 Microstructure of the WE43 and Mg-Zr magnesium alloys after ECAP a) WE43 after the 1st pass, b) Mg-Zr after the 1st pass, c) Mg-Zr after the 3rd pass

4. CONCLUSIONS

On the basis of the obtained results it is possible to draw the following conclusions:

- After ECAP processing the fined grained microstructure of the alloys AZ31, WE43 and Mg-Zr was achieved.
- The maximum value of strengthening in the case of AZ31 alloy (measured by hardness HV5) was reached at the 1st pass. At the 2nd pass this value decreased and after the 3rd pass it remained at approximately same level.
- The strengthening in the case of the alloy WE43 was more significant than in the case of the alloy AZ31.
- The ECAP process of magnesium alloys was the first time applied on new developed die for magnesium alloys. Microstructure of initial state of the Mg-Zr alloy is formed by large polyedric grains of Mg based solid solution with dimensions in the range of 100 – 500 μm.
- Maximum value of strengthening is reached at the 1st pass. At the 2nd pass this value decrease and continue to the 3rd pass approximately on the same level.
- Metallographic evaluations microstructures of the Mg-Zr alloy have also confirmed more intensive refining of grains already after the 1st pass.

5. REFERENCES

[1] ASM Handbook No.2, Properties and Selection: Nonferrous Alloys and special – Purpose Materials, ASM International, Metals park Ohio, 1990, p. 29

[2] Baker, H.: ASM Specialty Handbook. Magnesium and Magnesium Alloys, ed. Avedesian, ASM International, The Materials Information Society, USA, 1999

[3] Dobrzański, L.A.,Tański T., Čížek L.: Influence of modification with chemical elements on structure of magnesium casting alloys. Proceedings of 13th International Scientific Conference “Achievements in Mechanical and Materials Engineering” AMME’2005, Gliwice – Wisla, 2005, p.99-202

[4] Čížek L., Greger M., Pawlica L.,.Dobrzański L.A., Tański T.: Study of selected properties of magnesium alloy AZ91 after heat treatment and forming, Journal of Materials Processing Technology, 157-158, 2004, p. 466-471

[5] Hadasik E., Kuc D., Mikuszewski T.: Plasticity and microstructure of Mg-Li alloy, Metallurgy-News, 78, 8, 2011, p.617-621

[6] Inwahashi, Y., Wang, J., Horita, M., Nemoto, Z. and Langdon, T. G Principle of equal–channel angular pressing for processing of ultra–fine grained materials, Scripta Materialia, vol.35, 1995, p.143-147

[7] Rusz S., Final Technical Report of the Project GAČR No. 101/08/1110, 2011.

[8] Inwahashi, Y.,Wang, J., Horita, M., Nemoto, Z. Principle of equal–channel angular pressing for processing of ultra–fine grained materials, Scripta wMaterialia, vol.35, 1995, p.143-147 Materialia, 64 (2011), p. 355-358.

[9] Srinivasan R., Chaudhur, P. K., Cherukuri, B., Han, Q., Swenson, D., Gros, P. Continuous Severe Plastic Deformation Processing of Aluminium Alloys, Final Technical Report, DOE Award Number: DE-FC36-01ID14022, 2006, p. 1- 68.

[10] Drápala J., Kuchař L., Tomášek K., Trojanová Z.: Magnesium, its alloys and binary systems magnesium–admixture, VŠB-TU, Ostrava 2004

Acknowledgments

This paper was created within the project "**Creation of an international scientific team and incorporation to scientific networks in the area of nanotechnology and unconventional forming material. CZ.1.07/2.3.00/20.0038"**, which is financed by the European Social Fund and state budget of the Czech Republic.

european social fund in the czech republic
EUROPEAN UNION
MINISTRY OF EDUCATION, YOUTH AND SPORTS
OP Education for Competitiveness
INVESTMENTS IN EDUCATION DEVELOPMENT

Grain boundary engineering beyond adjusting special CSL boundaries – is SPD-processing a way to go?

G. Wilde

Institute of Materials Physics, University of Münster, 48149 Münster, Germany

E-mail: gwilde@uni-muenster.de

Abstract

The effect of thermal annealing on the microstructure evolution in nickel of 99.6 wt.% purity, severely deformed by Equal Channel Angular Pressing (ECAP) using the route B_C 4, was investigated. The ultrafine grained microstructure was shown to be characterized by numerous deformation bands with an average grain size of about 250 nm. High-temperature annealing induces heterogeneous recrystallization and grain growth. Though, some small grains are found to persist recrystallization in spite of pronounced grain growth in surrounding regions. This stability is suggested to be affected by specific microstructure elements containing rotational defects with a misorientation gradient of about 10° /µm along the band direction and thus perpendicular to the bounding high-angle interfaces. Pinning by orientation gradient prohibits motion of bounding interfaces and thus consumption of the grain by recrystallizing matrix.

1. INTRODUCTION

At small grain sizes, grain-boundary (GB) mediated processes that take part in accommodating externally applied mechanical stresses become more pronounced. Inherently, this leads to a stronger localization of the deformation, since only a fraction of the GBs are active and since the GBs are not acting as a homogeneous medium, but show pronounced spatial selectivity concerning the occurrence of stress-accomodating processes. When grain-boundary accommodated plasticity in terms of GB sliding is invoked, then in addition to the strong localization, inherent accommodation problems must be considered whenever the applied strain rate is incompatible with diffusional accommodation in/near the GBs. Additionally, the strong localization coupled to the accommodation problems seems to lead to stress concentrations that enable/force dislocation emission at all grain sizes that are achievable in real materials. At even higher strain rates, cracks form as seen in Molecular Dynamics simulations [1]. Similarly, if the plastic accommodation propensity of a material is exhausted by going to too fine grain sizes and/or too high defect densities, crack formation might result anyway, even at small strain rates [2].

As indicated above, such accommodation problems also lead to inhomogeneous distributions of the rigid-body rotation, which inherently causes rotational distortions inside grains and at the GBs [3]. In fact, through the occurrence of rotational defects inside the grains and at the GBs coupled to the geometric accommodation problems of any rigid body rotation in a grain ensemble containing GBs, Triple Junctions and Quadruple points, the kinetic stability of the microstructure against coarsening might be enhanced [3]. That hypothesis is based on the observation of strongly non-uniform grain

CZ.1.07/2.3.00/20.0038

size distributions in severely deformed material that had been nanocrystalline initially and also on the observation of microstructural locks in nanocrystalline material after severe deformation [3]. Especially rotational defects can be very efficient in hindering GB motion. Thus, in cases where such microstructural “locks” determine the temporal evolution of the average grain size, rotational defects might enhance the thermal stability of highly defected microstructures. It should be noted however, that such mechanisms can only be thought of as operative if the defect density is very high and it also results from the above concerning the localization and the inherent spatial heterogeneity that the stabilization would not effect the entire grain structure homogeneously but that regions of enhanced stability would neighbor regions where due to lower local defect density the stability would be unaffected.

After the initial observation of such microstructural locks presented by rotational gradients via HRTEM with subsequent analyses of the in-plane components of the strain tensor by Geometric Phase Analysis [3], this observation has now also been confirmed on the scale of the microstructure utilizing in-depth electron backscatter diffraction (EBSD) analyses, as indicated below.

2. EXPERIMENTAL PROCEDURES

UFG nickel specimens were prepared from cast nickel of 99.6% purity by equal channel angular pressing (ECAP). The route B_C4 was used where four ECAP passes are employed and the specimens are rotated by 90 degrees in the same direction in between the passes. The rods with a cross section of 10 × 10 mm^2 were deformed at room temperature and no back pressure was applied. As a result, an ultrafine microstructure was produced. The microstructure was characterized by scanning electron microscopy (SEM) using a FEI Nova NanoSEM 230 device. EBSD was used to identify the grains and to determine the grain misorientations. In order to follow the microstructure evolution caused by heat treatment, overall six areas, distributed over the whole cross-section of a Ni sample, were marked by Pt deposition in a way that they could be found after re-mounting of the specimen. An example of one such area is given in Fig. 1a. The SEM image was recorded and the EBSD analysis was performed for the squared area depicted by the green box in Fig. 1a. The resulting orientation imaging microscopy picture is shown in Fig. 1d. The identified grains are colored according to the inverse pole figure shown as insert in Fig. 1f. Subsequently, the specimen was subjected to a heat treatment at 700 K for 17 hours in argon atmosphere. Under these annealing conditions, the fraction of the recrystallized areas was found to occupy about 50% of the initial UFG microstructure [4]. After annealing, the same areas were inspected again and the corresponding SEM and OIM images were recorded (an example is shown in Fig. 1b and Fig. 1e, respectively). The same procedure was then repeated by annealing the sample at 750 K for 17 hours, and Figs. 1c and 1f represent the results for the same scanned area. It was proven that similar features were observed for all six inspected areas.

The microstructure was also examined by transmission electron microscopy (TEM) using a Zeiss Libra 200 FE field-emission microscope with an in-column Omega energy filter. Thin foils for TEM analysis were prepared by electropolishing using a solution of 17% perchloric acid in ethanol at 10.5 V and a temperature of −21 ◦ C.

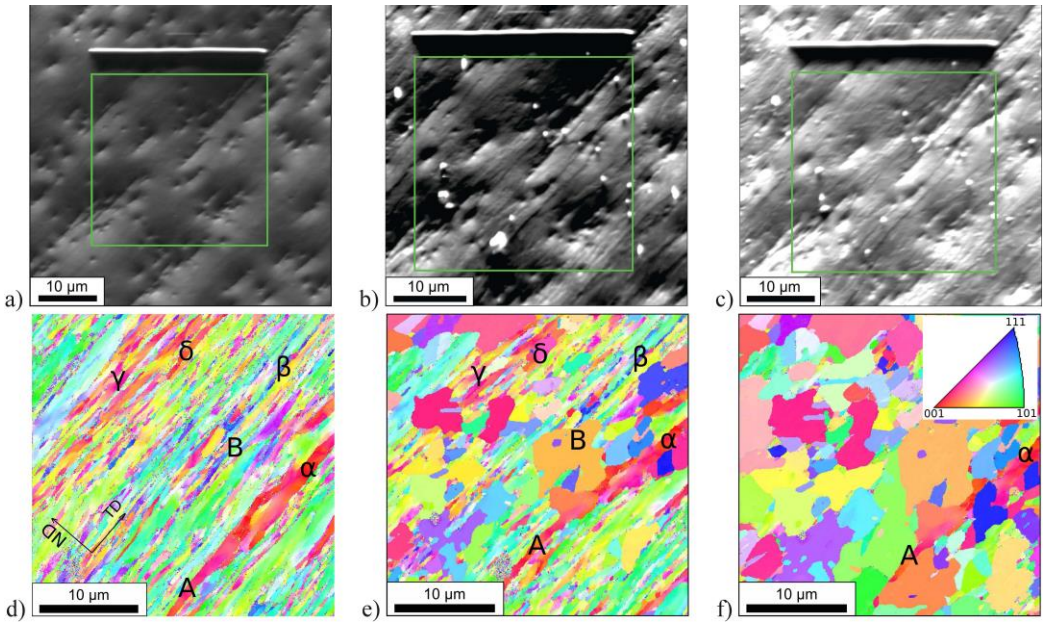

FIG. 1 SEM images of a polished surface of ECAP Ni with a deposited Pt wire that was used for localizing the same scanning area in the as-prepared state (a) and after annealing at 700 (b) and 750 K (c). The green boxes indicate the scanning areas analyzed by the orientation imaging microscopy in corresponding states (d–f). The grains are colored according to the inverse pole figure coding indicated as insert in (f). TD and ND are the transverse and normal directions, respectively. Areas, which are stable (**A**) and unstable (**B**) against coarsening are exemplary indicated. Areas, which were analyzed in detail, are indicated by Greek letters α, β, γ, and δ.

3. RESULTS AND DISCUSSION

UFG Ni prepared by ECAP via the route BC4 is characterized by an anisotropic and heterogeneous microstructure, Fig. 1d. Multiple deformation bands can also be distinguished with very fine and more equiaxed grains. TEM bright-field and dark-field images show orientation variations within elongated grains along the deformation bands, as represented in Fig. 2. In the bright-field (Fig. 2a), elongated grains with predominantly straight and flat interfaces are observed. Orientation changes along grains lead to contrast variations which occur even more clearly in the corresponding dark-field image using a crystallographic reflection (Fig. 2b). Similar orientations show similar brightness (compare features indicated by the two types of arrows in Fig. 2b). Additionally, a small-angle grain boundary (indicated by the dash-dotted line) is identified. A translation/rotation of the adjacent grains leads to a regular shift in the contrast along this interface. A dark-field image taken off any crystalline reflection (Fig. 2c) enhances the contrast arising by localized strain fields. Thus it can be concluded that dislocations lead to nonperiodic and localized contrast changes that are distributed within grains and along grain boundaries. A fuzzy and not straight interface (marked by the arrow in Fig. 2c) shows a high density of crystalline defects with some very localized contributions of moiré patterns. It should be noted that the observed contrast change (from bright to dark in Figure 2) is sensitive to orientation changes. Therefore, dislocation arrangements easily give rise to a gradual change of the orientation as detectable using the EBSD method. The average size of grains belonging to the deformation bands is estimated to be about 200 to 300 nm. The deformation bands are typically parallel to the transverse direction (TD) of the last ECAP pass indicated in Fig. 1d.

In addition to these very fine grains, there exists a microstructure fraction which is characterized by larger grains with significantly more anisotropic shape, Fig. 1d. Such grains are typically 0.5 to 1µm wide in the normal direction and at least several micrometer long along the transverse direction.

The formation of the deformation bands in UFG materials is an effect of the localization of the deformation [5, 6]. Adiabatic propagation of bands results in a partial recovery of the microstructure and a decrease of the dislocation density [7, 8]. Still, the deformation bands contain very fine grains, Figs. 1d and 2a. For subsequent analyses, we will distinguish the UFG microstructure fraction within the shear bands and the residual part which is relatively 'coarse-grained'. Inspection of the microstructure components, Fig. 1d, indicates that the change of colors is more diffuse in deformation (shear) bands and almost abrupt in the coarser component. This fact suggests that dislocations are organized into extended defects in the former with relatively smooth orientation gradients, whereas numerous dislocation walls (low-angle boundaries) dominate in the latter.

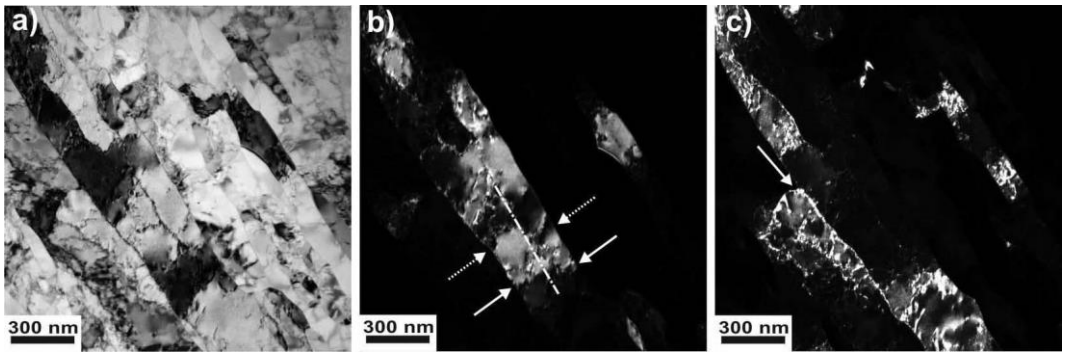

FIG. 2 TEM of ECAP Ni. (a) In the bright-field image elongated grains with predominantly straight and flat interfaces are observed. (b) In the corresponding dark-field image using a crystallographic reflection a particular crystallographic orientation shows up bright. Similar orientations (see two types of arrows) along a small-angle grain boundary (dash-dotted line) are indicated. A translation/rotation of the adjacent grains leads to a shift in the contrast along this interface. (c) A dark-field image taken off any crystalline reflection (contrast enhanced). Nonperiodic and localized contrast changes due to dislocations that are present and distributed within grains and along grain boundaries are observed. A fuzzy and not straight interface (marked by an arrow) shows a high density of crystalline defects with some very localized contributions of moiré patterns.

The effect of the annealing treatment on the microstructure evolution is investigated by ex-situ observation of the same area on the polished surface of the specimen. Annealing at 700 K induces heterogeneous recrystallization and abnormal grain growth in the UFG microstructure of ECAP Ni. A salient feature is that the changes occur to their large extent in the coarse-grained fraction of the initial UFG microstructure, Fig. 1e, while some fraction of the shear bands with smaller grains could still be well recognized. The used color coding allows following the changes in grain orientations. The effect is at a first glance unexpected – the smaller grains should have seen a higher deformation level and be more prone to grain growth and recrystallization. The stability of grains belonging to the shear bands cannot be explained by a hypothesis that re crystallization first occurs in the finer matrix component and then, due to a large density of the growing nuclei, their subsequent growth would be hindered. In such a case, a distinct change in the local orientations of the small grains belonging to the deformation bands would be expected. Contrary to that, Figure 1 suggests that there are fine stable fragments in the microstructure component (with respect to both, size and orientation) related to the shear bands and the grains in the coarse-grained UFG component growth further, e.g., compare regions A and B in Figs. 1d and 1e.

A comparative analysis of Figs. 1d–f allows to identify the specific features of the UFG microstructure which are exceptionally stable against recrystallization and grain growth. A number of microstructure elements, which represented initially deformation bands and revealed stability (e.g. α, β, and γ in Fig. 1d,e) or grew (δ) under the heat loading, were inspected. Similar features were found for the stable elements. For example, one of such defect configurations, α, corresponds to

grain lamellae of 150 to 250 nm thickness with a gradual change in orientation in the direction parallel to the lamellae boundary. The pointto-point and point-to-origin misorientation as a function of position for such a configuration (traced by the black line in the corresponding OIM images, Fig. 3a–c) are shown in Fig. 3d. The 'point-to-point misorientation' corresponds to the value of the misorientation angle between two successive points for the given line scan and the 'point-to-origin misorientation' represents the accumulated misorientation with respect to the first point of the given line scan. In both cases the value of the misorientation angle, irrespective to the misorientation axis, is plotted as a function of scan distance.

The analysis in Fig. 3a–d verifies the enhanced stability of the given microstructure fragment against thermal annealing even at 0.4Tm (here Tm is the melting point) in severely deformed Ni. The misorientation gradient, about 10°/μm, remains mostly unchanged after annealing at 750 K or 0.43Tm, too, although a slight increase of the slope towards the formation of a boundary can be suggested, Fig. 3d.

The microstructural elements providing the extreme stability against grain growth were analyzed in more detail. A large number of grains was found in the inspected areas which survived the annealing treatment at 700 K. The typical transverse size of such band-like fragments is about 200 nm. Their detailed inspection is difficult due to inherent limitations with respect to orientation resolution by the current EBSD analysis with the step size of 30 nm. The salient feature is a diffuse character of color variation along such bands in the OIM image that indicates a gradual misorientation within the given resolution limits.

Thus, the given stable microstructure fragment is represented by a bent and elongated grain with a rotational defect resulting in a misorientation gradient of about 10°/μm. In the 2D section, the rotational axis is almost perpendicular to the band/neighborhood interfaces resulting in a twist grain boundary. A second rotational component with the axis lying in the interface might be anticipated that produces an additional tilt misorientation component. However the latter may also be an artifact caused by the inclination of the band with respect to the inspected section.

The pinning by an orientation gradient is to be considered as a specific pinning mechanism which can act additionally to other known mechanisms and provide an additional stabilization of the ultrafine grained or nanocrystalline microstructure against grain growth under thermal loading conditions. This effect is related to the existence of specific rotational defects in the severely deformed matrix as it was also previously observed in HPT processed nanocrystalline Pd by high-resolution TEM of a specific triple junction – quadrupole junction configuration [3].

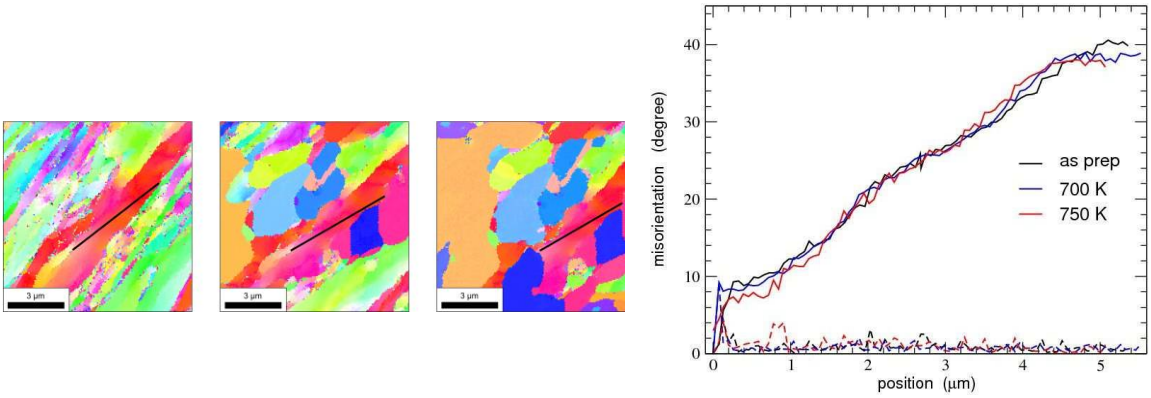

FIG. 3 The OIM images of the same microstructure fragments in the as-prepared state (a), and after annealing at 700 (b) and 750 K (c) for 17 hours. The black lines indicate the positions where point-to-origin (solid lines) and point-to-point (dashed lines) misorientations were traced, presented as function of position in (d).

The existence of such rotational defects limited by highangle grain boundaries prevents likely the microstructure element from coarsening as it is indicated by a careful inspection of the SEM data. An establishment of a quantitative correlation between the grain stability and the local misorientation parameters requires an additional intensive work which is out of the scope of the present paper.

4. CONCLUSIONS

The microstructure evolution in ECAP Ni is investigated as a function of annealing temperature. Pt deposition and orientation imaging microscopy were applied to follow the changes in the same area.

Recrystallization and subsequent grain growth were found to start in the UFG component which is characterized by a relatively larger grain size and presumably higher stored energy (higher dislocation density), whereas the shear bands with significantly smaller grains occurred to reveal an enhanced stability against the thermal loading [9].

Specific microstructure configurations in UFG Ni were found which can survive even an annealing at 750 K for 17 hours while the residual grains were subject to recrystallization and grain growth and reached sizes of 10 μm and larger.

Deformation bands are related to the existence of specific short-circuit paths of enhanced diffusion in ECAP Ni.

5. REFERENCES

[1] A Cao, Y Wie, Phys Rev B 76; 2007:024113

[2] Divinski SV, Padmanabhan KA, Wilde G, Phil. Mag. 2011; 91: 4574-4593

[3] H. Rösner, C. Kübel, Y. Ivanisenko, L. Kurmanaeva, S.V. Divinski, M. Peterlechner, G. Wilde, Acta Mater 2011;59:7380.

[4] V.V. Popov, E.N. Popova, D.D. Kuznetsov, A.V. Stolbovsky, E.V. Shorohov, G. Reglitz, S.V. Divinski, G. Wilde, Mater Science Engineer A 2013;585:281.

[5] Zhang HW, Huang X, Pippan R, Hansen N. Acta Mater 2010;58:1698.

[6] Hafok M, Pippan R, Phil Mag 2008;88(12):1857.

[7] M.A. Meyers, A. Mishra, D.J. Benson, Progress Mater Sci 2006;51:427.

[8] L. Hollang, K. Reuther, S.R. Dey, E. Hieckmann, and W. Skrotzki, Mater Sci Forum 2011;683:193.

[9] Divinski SV, Reglitz G, Wegner M, Peterlechner M, Wilde G, J. Appl. Phys 2014; in press.

Acknowledgements

The author is grateful for severe plastic deformation treatments performed in the groups of Prof. R.Z. Valiev (USATU, Ufa, Russia), Prof. Y. Estrin (Monash University, Clayton, Australia), Prof. R. Pippan (Erich Schmid Institute, Leoben, Austria) and Prof. M. Zehetbauer (University of Vienna, Austria). The author also acknowledges the financial support by the Deutsche Forschungsgemeinschaft (DFG).

This paper was created within the project "**Creation of an international scientific team and incorporation to scientific networks in the area of nanotechnology and unconventional forming material. CZ.1.07/2.3.00/20.0038"**, which is financed by the European Social Fund and state budget of the Czech Republic.

european social fund in the czech republic
EUROPEAN UNION
MINISTRY OF EDUCATION, YOUTH AND SPORTS
OP Education for Competitiveness
INVESTMENTS IN EDUCATION DEVELOPMENT

Effect of initial structure condition on UFG structure formation in low carbon steel

Jozef ZRNÍK[a], Sergey V. DOBATKIN[b], George RAAB[c], Libor KRAUS[a]

[a]*COMTES FHT Inc., Průmyslova 995, 33441 Dobřany, Czech Republic, jzrnik@comtesfht.cz*
[b]*Baikov Institute of Metallurgy & Materials Science, RAS, Moscow, Russia, dobatkin@ultra.imet.ac.ru*
[c]*Institute of Physics of Advanced Materials, UFA, Russia, G.I. Raab@mail.rb.ru*
[a]*COMTES FHT Inc., Průmyslova 995, 33441 Dobřany, Czech Republic, lkraus@comtesfht.cz*

Abstract

The paper focuses on the severe plastic deformation (SPD) of low carbon (LC) steel AISI 1010 (ČSN 12014) performed at increased temperature. The grain refinement of ferrite structure is monitored and described with respect to different initial structure of steel modified by solutioning and thermomechanical (TM) treatment prior severe plastic deformation. The refinement of coarse initial ferrite structure with grain size of 30 - 50 μm resulted from solutioning was then conducted in two steps. Preliminary structure refinement of coarse ferrite structure has been achieved due to multistep open die forging process and quite uniform ferrite structure with grain size of the order of 5 μm was received. In the second step grain refinement of steel structure was accomplished during warm Equal Channel Angular Pressing (ECAP φ= 120°) at 300°C, introducing the effective strain in range of ε_{ef} = 2.6 - 4. The change of microstructure in dependence of effective strain was evaluated by SEM and TEM study of thin foils. The high straining of steel resulted in extensive deformation of ferrite grains and formation of mixture of submicron grain structure in deformed banded structure with dense dislocation network and with a prevalence of subgrains. The dynamic polygonization process, due ECAP increase temperature, modified the submicrocrystalline structure formation. Thereafter only indistinctive difference in structure refinement was observed, considering the different initial steel structure. Deformation behaviour in condition of tensile strain was characterized by strength increased followed by consequent softening. For all states of steel, there was not observed uniform work hardening effect.

Keywords

Low carbon steel, thermal and thermomechanical treatment, SPD, ECAP, structure, mechanical properties.

1. INTRODUCTION

Ultrafine grained structures prepared by severe plastic deformation are receiving increasing attention in the technical community in the last years. The term “ultrafine grain structure” is referring to nanostructure with grain size of less than 100 nm, and submicrocrystalline structure with grains between 100 and 1000 nm. The fabrication of bulk materials with ultrafine grain sizes has attracted a great deal of attention over the past two decades because of the materials’

enhanced properties [1-3]. In recent years, it has become a worldwide effort to develop a manufacturing process to obtain ultrafine grain structures in steels. Currently, there are two main approaches for refining ferrite grains down to the ultrafine grain range in bulk steels. While the first group comprises advanced thermomechanical processes [4-7], the approach of the second group employs various sever plastic deformation techniques, including ECAP [1, 8], high pressure torsion (HTP) [9], accumulative roll bonding (ARB) [10, 11], constrained groove pressing (CGP) [12], to refine the structure by introducing the large plastic strain into bulk material.

In the present study, the modification of ferrite microstructure due to thermomechanical (TM) processing is described. Subsequently the effect of ferrite structure modification on development of ultrafine grain microstructure resulting from warm SPD was investigated and is assessed comparing with UFG structure resulted at SPD of conventionally treated AISI 1010 steel. The underlying relationship between microstructure and mechanical properties of the steel is reviewed.

2. MATERIAL AND EXPERIMENTAL PROCEDURES

For experimental the commercial low carbon steel AISI 1010 was used. The chemical composition of the steel in wt. % is as follow: 0.1 C, 0,42 Mn, 0,18 Si, 0,024 P, 0,018 S. Prior to ECAP pressing a conventional solutioning treatment of steel billets was carried out at the temperature of 920°C for 1 h, followed by air cooling. The microstructure, documented by SEM, resulted from solutioning is presented in - **Fig. 1a**. Subsequently, from thermally treated plates the cylindrical billets with initial diameter of 9 mm and length of 50 mm were cut off for the ECAP deformation experiment. By appropriate thermomechanical (TM) treatment, the coarse structure refining is advantageous and more suitable structure prior further grain refining. Refined structure can then provide better combination of strength, toughness and ductility without additional alloying of steel. Accordingly, in order to achieved prior ECAP pressing preliminary refinement of the solutioned steel a structure modification has been carried out in condition of TM treatment. After steel soaking at 900°C, cylindrical specimens in form of pegs, with initial diameter of 18 mm and length of 40 mm were subjected to compressive deformation [1]. The repetitive axial deformation of the peg between flat dies of hydraulic press performed continuously, without any further peg reheating, through the recrystallized,nonrecrystallized and inter-critical α + γ temperature region was expected to result in ferrite structure refinement. The last reduction of the peg was at temperature region of about 700°C. Among successive deformation reductions the specimen was rotated along the longitudinal axis until the final shape of specimens was acquired. Scanning electron micrograph of the resulting microstructure in the centre of the forged specimen cross section is shown in - **Fig. 1b**. The average ferrite grain size

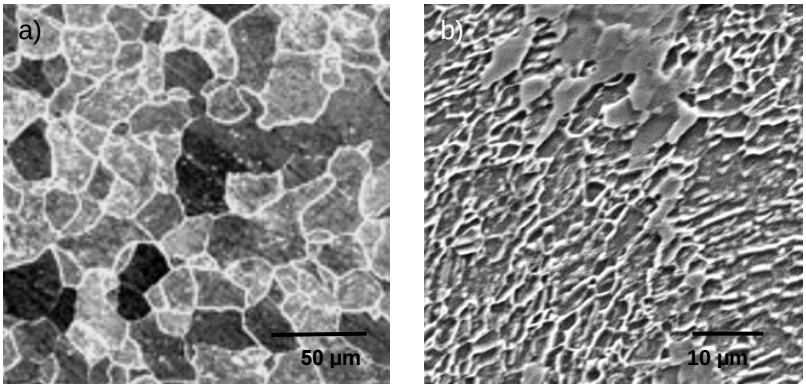

Fig. 1 Initial microstructure of solutioned and TM treated steel prior ECAP.

measured at areas of various compressive strains from near the surface to the centre of the peg was below 5 μm.

The ECAP pressing was performed at temperature of 300°C. The angle of intersection of the two channels (φ) was equal to 120°C. The ECAP die used for the experiment was heated to pressing temperature and held for 30 minutes. The samples (bars) prior ECAP pressing were heated for 300 s, which was done inside the pre-heated die until sample reached the pressing temperature. Each billet was pressed and experienced four, five and six passes (N) through the the die.

The effective strain corresponding to one pass through the die was ε_{ef} = 0.67. Six passes correspond to the total strain of ε_{ef} = 4. The each billet was rotated between the consecutive passes around its longitudinal axis by 90° in the same direction. This procedure is generally referred to as the processing route Bc. This deformation procedure was selected to deform samples because it enables the formation of homogeneously deformed microstructure. It was not considered that the stress generated in sample after each pass, would be recovered (static recovery) due to repeated reheatings of the billet inside the die prior the next pass will be carried out. The microstructural examination of thermally (TM) treated and ECAP deformed samples was conducted by SEM of bulk billets and TEM of thin foils. Thin foils for TEM investigation were sliced from ECAP deformed billets normal to their longitudinal axis. The SEM and TEM microstructures were obtained by using JEOL JSM 6380 SEM microscope, operating at 10kV and JEOL JEM 200FX TEM operating at 200 kV. Selected area diffraction was used to investigate a progress in ultrafine grain transformation in dependence the strain value introduced.

Wicker hardness and tensile tests were carried out using MTS universal testing machine equipped with Multisens extensometer. Tensile specimens with gauge length of l_o = 30 mm were tested at a constant cross-head speed of 0.016 mm/s until failure. The engineering stress-strain curves were constructed.

3. EXPERIMENTAL RESULTS AND DISCUSSION

3.1 Microstructure of solutioned and ECAP processed steel

The ferrite structure, resulted when applied only solutioning at 920°C, was found uniform across the billet and also as concerns the grain size and morphology, is presented in Fig. 1a. Scarcely, the cementite particles were found deposited along grain boundaries. The mean size of ferrite grains was measured in the size range of 30 to 50 μm. Microstructural characteristics in ECAPed deformed, prior only solutioned samples, exposed to different straining for the chosen

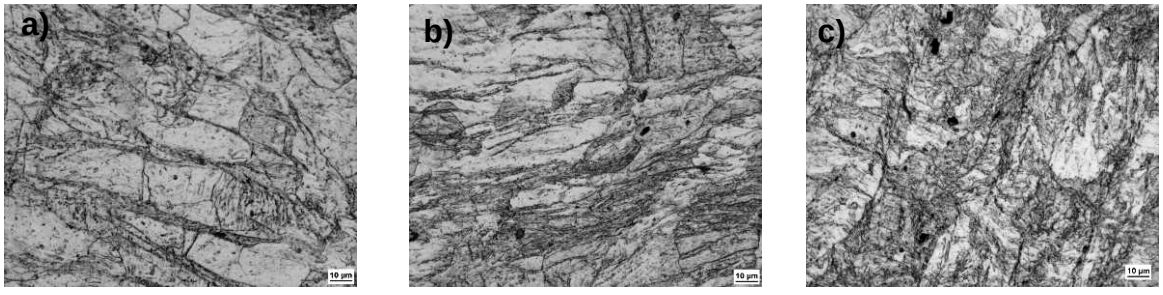

Fig. 2 Deformed microstructure across the billet resulted from solution treatment and different ECAP straining: a) N-4 passes; b) N-5 passes; c) N-6 passes.

processing route Bc, were analysed in detail on section normal to longitudinal axis of deformed billets. Representative micrographs of deformed ECAP-ed steel, when processed by only solutioning treatment prior ECAP, were taken on X plane, which was perpendicular to bar axis are presented in **Fig. 2**. Each structure represents the effect of different straining (number of passes) the steel was exposed to. Light microscopy micrographs of the structure as-pressed billets to different strain provided evidence of effective straining as to formed deformation features of formerly coarse initial steel ferrite structure.

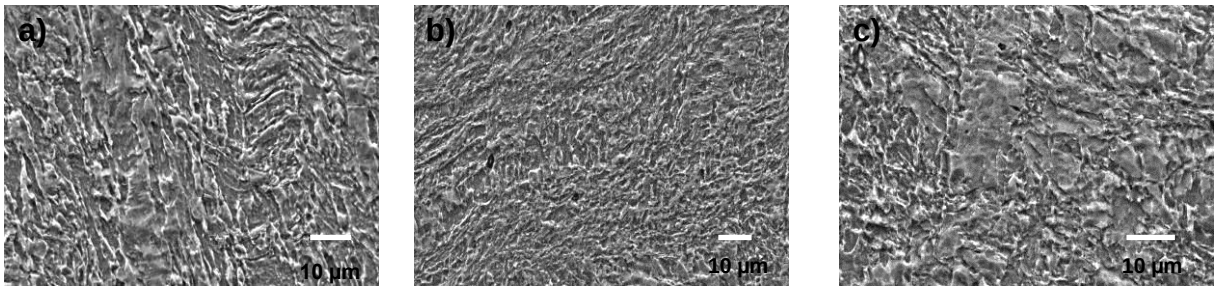

Fig.3 Deformed microstructure across the billet resulted from solutioning and TM treatment prior ECAP straining a) N-4 passes; b) N-5 passes; c) N-6 passes.

3.2 Microstructure of prior thermomechanically treated steel and ECAP processed steel

Deformation characteristics, regarding the initial structure condition, either only solutioning and/or solutioning followed by TM treatment, and applied strain level ε_{ef}, provided evidence on deformation structure heterogeneity distribution resulting from introduced varying straining across deformed billets resulted in forming of localized deformed bands. In refined ferrite structure due to preliminary TM treatment, the prior coarse initial ferrite structure, resulting from only solutioning, was however refined, as can be seen in **Fig. 1b**. Then, when introduce ECAP straining, no matter the strain level was, the structure heterogeneity as regards subgrains formation and grains refining in deformed structure was resulted and observed**, Fig. 3**. Deformation localization and banding in ferrite structure was increasing as number of passes increased. However, as increasing straining ε_{ef} then deformation bands became more frequent in structure and distributed in more dense manner, as can be seen in **Fig. 3 b,c.** In the structure, which was refined by TM treatment prior ECAP deformation the structure heterogeneity was detectable as well. However, there in differently deformed areas due to appearance of strain distribution heterogeneity differently deformed areas appeared. In deformed bands where shearing effect was evident the grain refinement appears to be effective to support fragmentation of deformed grains due to effective shearing. These microstructures are evidence that transformation process of ultrafine structures tends to be more efficient in TM refines structure. Structure deformation by ECAP, regardless the strain applied and the initial structure of steel was of coarse or refined condition. In the structure as result of the deformation heterogeneity the areas where structure was only softy deformed and equiaxed grains were found. Performing N=5 and 6 passes the deformation banding was more dense and within this bands the dense dislocation network and dislocation cell structure was formed. Not regularly, but inside the bands the fragmentation of elongated grains starts as result of slipping process.

The results suggest, using the die having channel angle of φ =120° the higher straining is needed to obtained homogeneous deformed structure when formation of ultrafine grain structure might be received. However, the TM preliminary treatment of steel contributes by only small deal to deformation homogeneity and structure refinement at deformation.

3.3 ECAP ultrafine microstructure prior modified by solutioning and TM processing

Microstructure analysis by SEM provided the evidence on applied effective strain, that was not efficient to deform structure of steel sufficiently and uniformly across and along the billet, regardless the initial structure was coarse and then refined by TM treatment prior ECAP deformation. In order to receive more detailed information on structure refinement and structure formation in steel having different initial structure the transformation process was also investigated by TEM and more detailed information on mechanism of structure transformation were received. The substructure development characteristics provided by TEM analyses of thin foils showed more details as regards the mechanisms, which governed the structure transformation in severely deformed areas (shear bands) of billets. The development of deformed substructure in steel having different initial microstructures and subjected to different straining is shown as collection of substructures in **Fig. 4.**

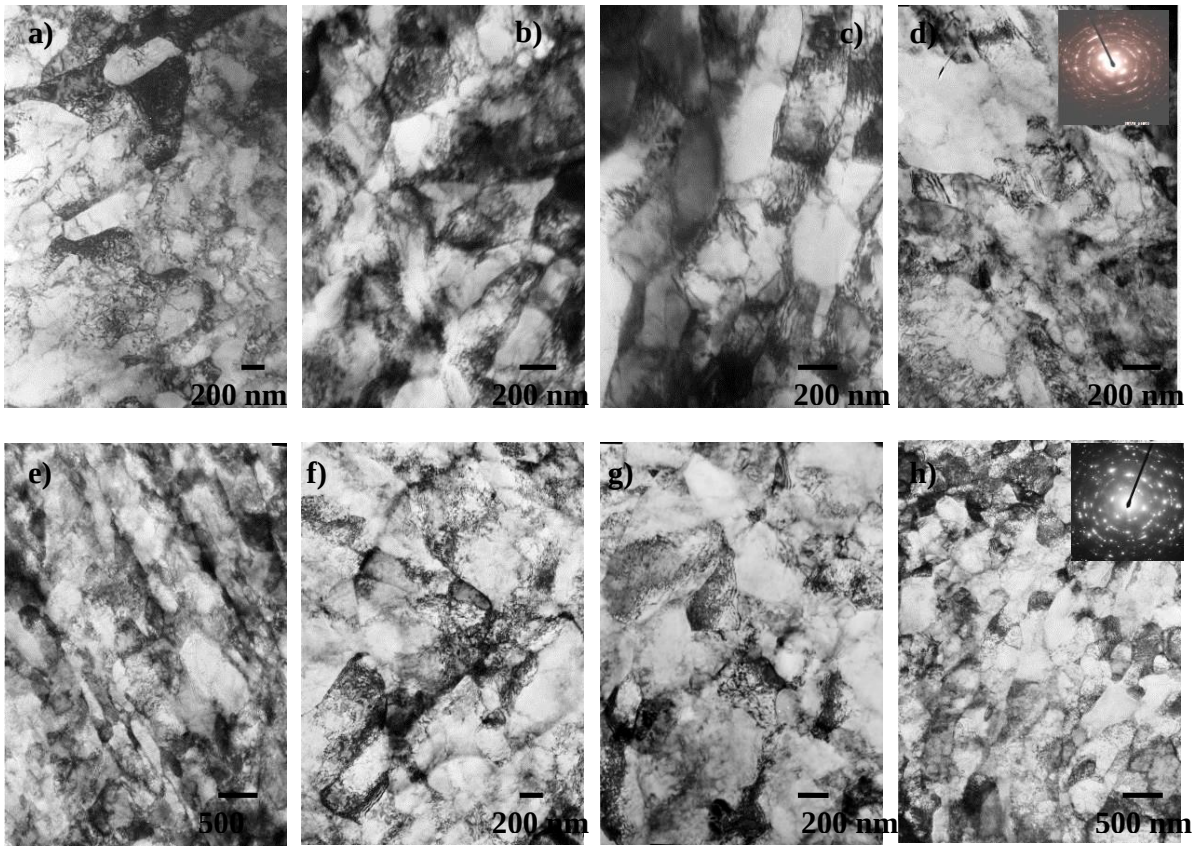

Fig.4 TEM micrographs developed in prior solutioned and/or solutioned and TM treated steel subjected to ECAP straining experience N-4,5 and 6 passes. Solutioning exposed samples: a,b,c,d, and TM exposed samples: e,f,g,h

The substructure developed in deformed billets subjected to warm ECAP at temperature of 400°C was investigated on plane parallel with billet longitudinal axis and substructure analyses provided the evidence on efficiency of deformation process for structure refinement in the same steel having different initial structure. These representative microstructures show and confirm the progress in ultrafine grained formation as straining increases.

Comparing effect of prior structure refinement of steel by TM processing there is not substantial difference observable in microstructure formation. At both initial structures, either coarse and/or prior refined by TM, the TEM analyzes did not identify the difference in structure characteristics. The deformation bands, which are formed during straining in deformed structure, consist of the elongated ferrite grains where dense dislocation and dislocation cell structure is build up, as can

be seen in Fig. 4 a,e. Considering the local straining heterogeneity in billet the microstructural evolution and fine structure development in deformed billet depends on the initial structure condition, the TM processing conditions of steel and on the selected local position of analyses. It is probably caused by accumulative straining resulted from both processes - TM process and ECAP deformation of steel. The local substructure modification across the deformed bars than varies locally. At both ECAP samples with increased straining (N= 5 an N= 6) dislocation activities can be related to progress of polygonization and nucleation of new subgrains within the elongated ferrite grains, as can be seen in **Fig. 4 b,c,f**. The specific fringe contrast along some subgrains boundaries and appearance of small grains fre of dislocations can be then attributed to local (in-situ) dynamic recovery and polygonization process. At increase temperature the influence of recrystalization effect can contribute to structure modification as well. The more developed small equiaxed grains having high angle boundaries and with less dislocation density inside were found for both steel states when subjected to N= 6 passes, as shown in Fig. **4 d,g,h**. More frequently were these grains found in steel, which was TM treated prior ECAP deformation The SAED patterns indicated an increase in the reasonable portion of boundaries having high angle misorientations. These results can be due to the fourfold effect, involving grain refinement, the ECAP processing temperature, strain introduced and latent heat generation at SPD, acted as an effective driving force for dynamic recrystallization process contribution to modify the deformed structure. The progress in ultrafine grain structure formation was more evident in deformed steel bars, which were preliminary TM treated prior ECAP processing. More effective structure refinement after ECAP can be caused by cumulative straining resulted from both processes, TM and ECAP and reaching then higher driving force for in-situ dynamic recovery and recrystalization processes.

3.4 Mechanical properties of steel

The mechanical properties of experimental steel, which was subjected to thermal and thermomechanical treatment prior SPD were measured by tensile test and hardness measurement. The results of tensile testing performed at room temperature are shown in **Fig. 5**, which represents the initial solutioned structure, solutioning and ECAP and TM and ECAP treatment. In case of the initial annealed steel condition there is an extensive period of work hardening and large elongation to failure. The deformation curves corresponding to TM treated steel shows slight work hardening effect and shorter deformation to failure. The mechanical properties data for all structural states are stated in **Table 1.**

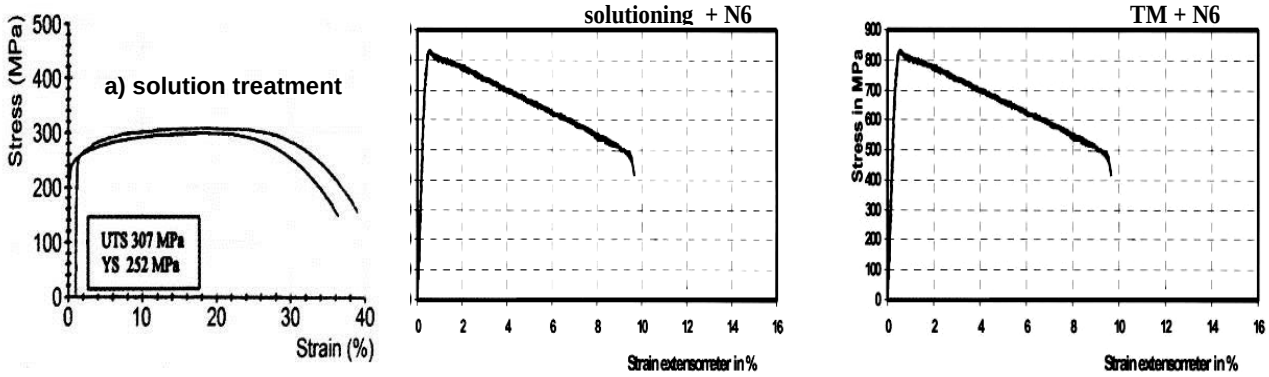

Fig. 5 Engineering stress-strain records: a) initially treated steel; b) solutioning and ECAP; c) TM treatment + ECAP .

The deformation behaviour of soaked and ECAP steel specimens is very similar for all structural states and/or three specimen, which have experienced different deformation. There is, after

reaching the yield stress, section of slight hardening increase, which is not modified as the straining is increased. On the other side the strength value is of the same level for all specimens, which can be incurred by explained by large deformation strengthening of ferrite, as could be seen in deformed structures.

Table 1 Mechanical properties of steel AISI 1010 after solutioning and after ECAP

stav	E [GPa]	$Rp_{0,2}$ [MPa]	Rm [MPa]	A_{tot} [%]	Z [%]	HV30
NŽ	-	245	303	37	81	101
N4	200	813	819	10,4	63	264
N5	191	763	768	9	60	260
N6	208	851	857	9	60	268

Table 2. Mechanical properties of steel AISI 1010 TM treated and after ECAP

stav	E [GPa]	Re_H Re_D [MPa]	Rm [MPa]	A_{tot} [%]	Z [%]	HV30
TMS	216	357 287	370	31	76	109
N4	224	811	815	10,8	58	320
N5	213	767	778	9,5	62	338
N6	210	824	833	10	54	379

4. EXPERIMENTAL RESULTS EVALUATION

When evaluating the progress in ultrafine grain structure development and mechanical characteristics with respect to strain introduced a conclusion can be expressed that there was not achieved a significant difference when comparing different initial state of structure in steel was prepared. Microstructural evolution process was only slightly modified as to the formation of deformed structure advancement with a certain level of strain introduced. TEM substructure analysis however provided the evidence that formation of ultrafine grained structure was a step forward when compared with initial coarse steel structure deformation process. However, deformation heterogeneity, which was observed higher in coarse grain structure, restrained consequentially the recovery and polygonization process in deformed structure. As the result of this postponement the formation ultrafine grains was subsequently delayed and smaller fraction of them was found in mixed deformed microstructure deformed to various strain. The contribution of this fact was detected also by small decrease of the strength value for TM treated steel where the more advanced volume fraction of ultrafine grains in microstructure cause slight drop in ultimate strength of steel. The level of deformation strengthening was still higher in coarse structure. Nevertheless the progress in structure refinement influenced only in small extent the mechanical behaviour of different steel states.

At final evaluation of deformation experiment it is important to state out that resulted strength values of experimental steel modified by intensive channel deformation reached the value, which was more then two times higher when comparing with values resulting from industrial heat treatment of low carbon steel. The drawback, however is the fact the lack of plastic deformation ability of severely deformed steel remains.

5. CONCLUSIONS

The low carbon steel AISI 1010 (ČSN 12014) was subjected to severe plastic deformation using ECAP die with aim to search the formation of ultrafine grain structure in dependence of the initial structure modification and straining at increased temperature. By SEM and TEM analysis and have been received the sufficient evidences about the progress on deformed structure state and mechanical properties modification.

6. REFERENCES

[1] V. M. Segal, V. I. Reznikov, A. F. Dobryshevski, V. I. Kopilov: Metaly, 1, 1981, IAN SSSR, 115-124.

[2] V. M. Segal: Mat. Sci. Eng. A, 197, 1995, 157.

[3] R. Z. Valiev, R. K. Islamgaliev, I. V. Alexandrov: Progr. Mateer. Sci., 45, 2000,103.

[4] P. D. Hodgson, N. R. Hickson, R. K. Gibss: Sripta Mater., 40, 1999, 1179.

[5] R. Kaspar, S. J. Distl, O. Pawelski: Steel Research, 59, 1988, 421.

[6] Y. Matsumara, Y. Yada: ISIJ Intern. 27, 1987, 492.

[7] A. Najafi-Zadeh, J. J. Jonas, S. Yue: Metallurgical Trans. A, 23, 1992,2607.

[8] R. Z. Valiev, A. V. Korznikov, R.R. Mulyukov: Fizika Met & Metalov.: 4, 1992, 70.

[9] R. Z. Valiev, R. K. Islamgaliev, I. V. Alexandrov: Progr. Mater. Science: 45, 2000, 103.

[10] Y. Saito, H. Utsunomiya, N. Tsuji, T. Sakai: Acta Materialia, 47, 2002, 579.

[11] N. Tsuji, R. Ujei, Z. Minamino: Scripta Mater., 47, 2002, 69.

[12] D. H. Shin, J. J. Park, Y. S. Kim, K. T. Park: Mater. Sci. Eng. A, 375, 2002, 178.

Acknowledgement

This paper was created within the project "**Creation of an international scientific team and incorporation to scientific networks in the area of nanotechnology and unconventional forming material. CZ.1.07/2.3.00/20.0038"**, which is financed by the European Social Fund and state budget of the Czech Republic.